Geology, Geochemistry, and Current Genetic Models for Major Mississippi Valley-Type Pb–Zn Deposits of Morocco

Mohammed Bouabdellah and Donald F. Sangster

Abstract

Morocco has been for the past two centuries one of the top ten Pb–Zn producers with two thirds of base-metal production derived from three major Mississippi Valley-type districts (Touissit-Bou Beker, Upper Moulouya, and Jbel Bou Dahar). Collectively, these districts have produced more than 100 Mt of ore at an average grade of ~3 wt% Zn and 4 wt% Pb. At the present time, none of the three districts is active. Economic orebodies are hosted by a succession of Lower to Middle Jurassic unmetamorphosed, platform carbonate rocks. The epigenetic and stratabound sulphide deposits occur as open-space fillings and metasomatic replacements of carbonate. Mineralization that fills open spaces (i.e., veins, interconnected cavities, solution-collapse breccias) accounts for most of the higher grade orebodies. Overall, the mineral paragenesis consists principally of variable proportions of sphalerite and galena, accompanied by different generations of saddle dolomite (Touissit-Bou Beker), calcite (Jbel Bou Dahar), or barite (Mibladen). In all of the districts, paleogeographic reconstructions indicate that the orebodies are located above basement topographic highs against which the Triassic and Early Jurassic formations pinch out. Regionally, ENE–WSW- and E–W-trending faults appear to have been a critical factor in ore genesis, having provided

M. Bouabdellah (✉)
Département de Géologie, Faculté des Sciences,
Université Mohammed Premier,
Avenue Mohammed VI, B.P. 717,
60000 Oujda, Morocco
e-mail: mbouabdellah2002@yahoo.fr

D.F. Sangster
Geological Survey of Canada, 601 Booth Street,
Ottawa, ON K1A 0E8, Canada

D.F. Sangster
Geological Survey of Canada, 2290 Relin Way,
North Gower, ON K0A 2T0, Canada

M. Bouabdellah and J.F. Slack (eds.), *Mineral Deposits of North Africa*,
Mineral Resource Reviews, DOI 10.1007/978-3-319-31733-5_19

favorable fluid channels for metal-bearing brines into permeable host rocks and dissolution structures. The geometry of the orebodies that parallel the major alpine faults, coupled with lead isotopic constraints, suggest that the MVT mineralizing event occurred during midle Tertiary time (i.e., Cretaceous to Miocene) coincident with closing stages of the Alpine orogeny in the Atlasic orogenic belt. Alpine mineralization is thought to have been promoted by the mixing of older, high-temperature, rock-buffered, dense brines stored within the Paleozoic basement, and a downwelling, cooler fluid probably of meteoric origin. The resulting mixed brines were centered mainly on the basement high structure and its flanks, then flowed laterally away from the basement high and giving rise to the lower grade mineralization of the distal prospects. Fluid migration towards the ore districts could have been achieved either by a gravity-driven system (Touissit-Bou Beker, Mibladen, and Jbel Bou Dahar) or sediment compaction in the foredeep (Jbel Bou Dahar), or a combination of both. An alternative buoyancy-driven fluid convection model is proposed for the Touissit-Bou Beker MVT mineralization.

1 Introduction

The Mesozoic to Cenozoic intra-continental Atlas system of Northwest Africa extends over a distance of 2000 km along strike from the Moroccan passive Atlantic continental margin to the Tunisian Mediterranean coast (Fig. 1). This system contains one of the most fertile Pb–Zn ± F ± Ba Tethyan-Atlantic metallogenic provinces as it is host to >1,000 Mississippi Valley-type (MVT) occurrences and deposits that range from small uneconomic showings to major districts of great size and productivity. This large province has been a world lead-zinc producer for at least 200 years, with an overall total production exceeding 20 Mt of combined Pb + Zn.

The Atlas system *ss* comprising the High and Middle Atlas in Morocco, the Saharian Atlas and Aurès Mountains in Algeria, and the Tunisian Atlas in Tunisia (Fig. 1) is attributed to the inversion of Jurassic rift or transtensional basins as a consequence of continental convergence between Africa and Europe during Cenozoic time (Jacobshagen et al. 1988; Beauchamp et al. 1996; Frizon de Lamotte et al. 2009). According to Leach et al. (2010), this interval of time included microplate assimilation that affected the western margin of North America and Africa-Eurasia and constitutes a favorable period worldwide during which approximately 36 % of dated MVT deposits formed.

In the Atlas system, economic Pb–Zn ± F ± Ba orebodies are enclosed within unmetamorphosed, flat-lying Mesozoic to Cenozoic shallow-water carbonate platform strata. These strata experienced multiple overlapping episodes of dolomitization, dissolution (i.e., karstification), and uplift during the Mesozoic breakup of the Pangean continental shelf of West Africa. There are no known Precambrian or Paleozoic examples of such orebodies. Among the major lithostratigraphic reservoirs, only three contain significant MVT mineralization, and all of these were important paleoaquifers during much of the evolution of the Atlas orogen. Indeed, more than 90 % of the exploited deposits and prospects occur within Lower and Middle Jurassic carbonates and, to a lesser extent, Triassic dolostones. Major deposits are concentrated in six separate mining camps, including in Morocco the word-class and historically important Touissit-Bou Beker district (>100 Mt at 4 wt% Pb, 3.5 wt% Zn, <1 wt% Cu, 120 g/t Ag; Bouabdellah et al. 2012, 2015), the Upper

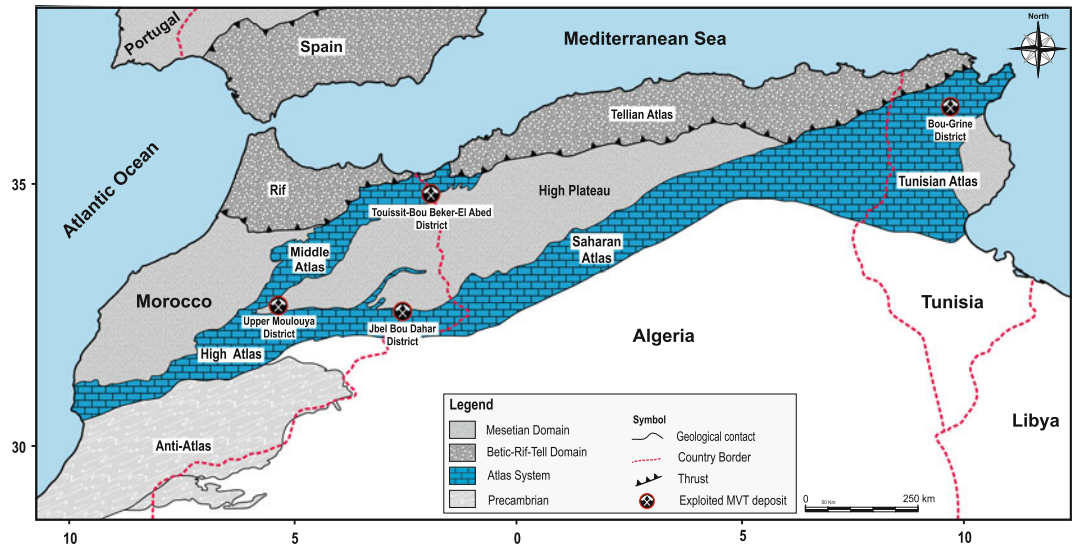

Fig. 1 Structural map of northwestern Africa and southern Iberia illustrating main lithostructural domains and spatial distribution of major Maghrebian (i.e., Moroccan, Algerian, and Tunisian) MVT districts within the Atlas system

Moulouya district (>30 Mt at 4 wt% Pb), and the Jbel Bou Dahar district (>30 Mt at 4 wt% Pb, 4 wt% Zn), the El Abed district in Algeria that constitutes the eastern termination of the Moroccan Touissit-Bou Beker district, and the Bou-Grine district and related deposits of the diapir zone in Tunisia (Fig. 1).

Extensive field, mineralogical, fluid inclusion, and isotopic studies during the last three decades have greatly improved our understanding of the genesis of MVT deposits in northwest Africa. However, in spite of abundant available geological, mineralogical, and geochemical data (Rajlich 1983; Dupuy and Touray 1986; Makhoukhi 1993; Bouabdellah 1994; Bouabdellah et al. 2012, 2015), the basic questions of genesis remain controversial with proposed models ranging from syngenetic to epigenetic. The lack of minerals suitable for radiometric age dating, together with the omnipresence of post-ore oxidizing events, have left the age of Pb–Zn mineralization as the subject of ongoing debate, and therefore any robust genetic model open to controversy.

The purpose of this paper is to (1) combine information on the most productive and best-studied MVT districts of Morocco for which production and reserve data are available; (2) review individual geological environments for these historically important base metal deposits; and (3) discuss the current new fluid inclusion and isotopic data, and proposed ore deposit models.

2 Touissit-Bou Beker District

The Touissit-Bou Beker district of northeastern Morocco and adjacent western Algeria (Fig. 2) is one of the top ten MVT districts in the world with a total production, over 75 years of mining activity, that exceeds 5 Mt of Pb + Zn. Production started in 1926 and ended in 2002 due to exhaustion of ore, decrease of ore grades with depth, and collapse of lead prices. Since 2002, however, limited-scale open-pit and associated subsurface artisanal mining is producing >10,000 t/years of ore averaging 6 % Pb.

The district (Fig. 2) is located within the northeastern part of "la Chaîne des Horsts" Atlasic belt, and covers an elongate, ENE-trending area of 64 km^2. Among the five mines that constitute the district, four are in Morocco (Mekta, Beddiane, Touissit, and Bou Beker) and one is in adjacent Algeria (El Abed).

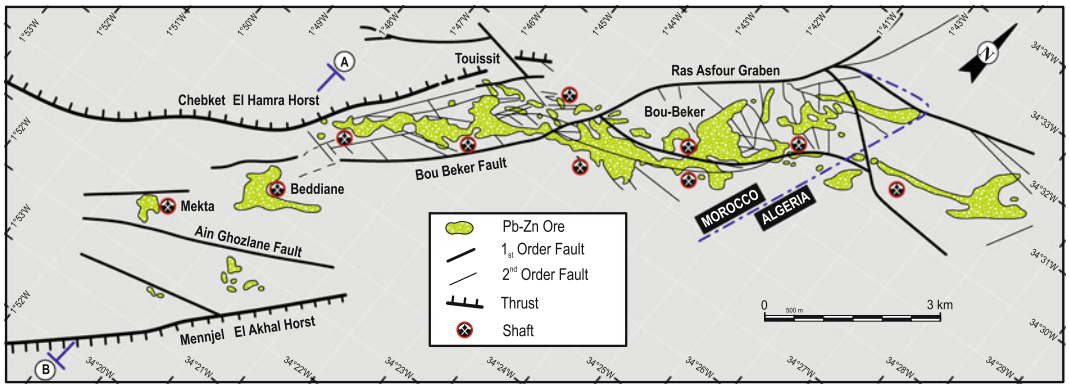

Fig. 2 Structural setting of Touissit-Bou Beker district showing exploited MVT orebodies projected to surface. Note that orebodies are elongate parallel to the main NE–SW fault system. Section line *A–B* indicates cross-section presented in Fig. 3

The Moroccan deposits, which occur in a primary envelope of Pb + Zn mineralization defined by a cutoff grade of 3 % Pb + Zn, differ from most MVT deposits owing to the dominance of lead over zinc, and locally (i.e., Beddiane deposit) to elevated concentrations of Cu (~1 %) and Ag (120 g/t). All of the exploited deposits are confined to a graben structure locally known as the Missouine graben (Fig. 2). Exploited higher grade lead-zinc orebodies are restricted to the Aalenian-Bajocian dolomite aquifer; making this tectonostratigraphic unit one of the most promising for MVT exploration in Morocco.

The summaries presented hereafter draw extensively from the recently published papers of Bouabdellah et al. (2012, 2015) as these constitute the most exhaustive and comprehensive descriptions published on this district.

2.1 Mining History

Discovered in 1926 and mined underground until 1973, the Bou Beker and Touissit deposits, the first operating underground mines in the district, were exploited by the European companies "la Société des Mines de Zellidja" and "la Compagnie Royale Asturienne des Mines," respectively. Between 1970 and 1980, widespread and intensive grid drilling along strike in the Missouine graben resulted in the discovery of the exceptionally high-grade Beddiane and Mekta deposits at depths of 110–180 m, respectively (Fig. 3). Calculated mean Pb grade for both deposits exceeded 10 % and locally reached 18 % (i.e., Hassi Msidira orebody; Bouabdellah et al. 2012). In 1980, the multinational "Compagnie Minière de Touissit" purchased the assets and began working the Mekta and Beddiane deposits.

2.2 Geological Setting

The geology of the Touissit-Bou Beker district has been well described by numerous investigations (Voirin 1965; Samson 1973; Touahri 1991; Rajlich 1983; Dupuy and Touray; 1986; Makhoukhi 1993; Bouabdellah 1994; Torbi and Gélard 1994; Ajaji et al. 1998; Aboutahir 1999; Bouabdellah et al. 1996a, b, 1999, 2001, 2012, 2015). Only a summary of the main conclusions relevant to the present study are given below.

Overall, the district stratigraphy consists of a Paleozoic basement unconformably overlain by a series of tabular and unmetamorphosed Meso-Cenozoic to Quaternary terranes (Fig. 4a, b). The Paleozoic rocks consist of weakly metamorphosed, Ordovician pelitic schists (Torbi 1996) locally intruded by porphyritic Visean rhyodacite. Unconformably overlying the Paleozoic basement is a thin lithostratigraphic unit made of a succession of basal

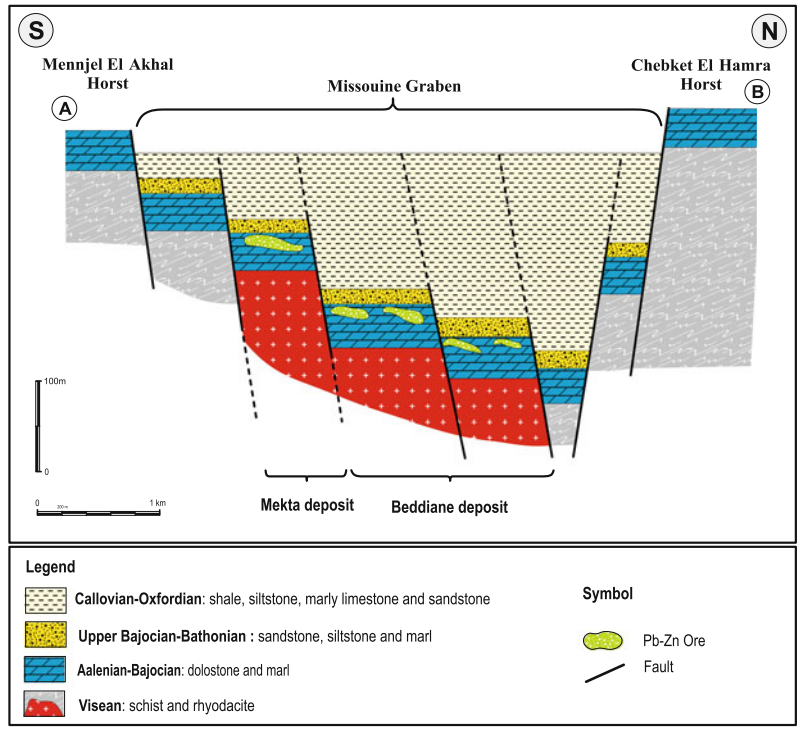

Fig. 3 Generalized N–S cross-section through Missouine graben showing position, at variable depths, of Mekta and Beddiane orebodies (see Fig. 2) relative to stratigraphy and facies units, and horst and graben structures with Middle to Upper Jurassic sedimentary infill

conglomerate and fine-grained limestone attributed to the Early Jurassic (Sinemurian-Carixian?). Paleogeographic reconstructions show that the Pb–Zn orebodies are located above an isolated topographically high carbonate platform of Paleozoic age known as the "Mole of Touissit" or "Touissit Shelf" (Samson 1973), against which the Triassic and Middle Jurassic formations pinch out (Fig. 5). The Aalenian-Bajocian (Middle Jurassic) carbonate sequence, which hosts nearly all economic deposits of the Touissit-Bou Beker district, rests either directly on the Paleozoic basement or conformably overlies the Early Jurassic unit. It consists of a succession of interbedded grey to brown, medium- to coarse-grained dolostone with thin (0.1 up to 1 m) layers of marl and clay, indicating a shallow sub- to intertidal, low-energy depositional environment. The 10–20-m-thick "Toit Jaune" unit constitutes the hangingwall rocks for the MVT mineralization and unconformably overlies the Aalenian-Bajocian dolostones (Fig. 4a, b). This unit consists primarily of a succession of yellow sandstone and silty shale interlayered with argillaceous carbonate, grading upward into a Bathonian regional stratigraphic marker made of a condensed succession (up to 2 m) of clay-rich siltstone and ammonite-bearing silty limestone with intercalated ferruginous oolitic beds. Overlying the Bathonian is a regionally developed organic-rich black shale up to 100 m thick that formed the "cap rock" during Pb–Zn mineralization. The host rocks are dissected by a series of faults, which regionally trend ENE–WSW and E–W, with a subordinate set that strikes NNW–SSE (Fig. 4). These fault structures appear to have played a critical role in ore genesis as they provided favorable fluid channels for MVT mineralization.

2.3 Alteration

Dolomitization is the principal type of wall-rock alteration. Two major stages have been distinguished based on petrographic, sedimentological, and isotopic (C, O, Sr) data (Bouabdellah 1994; Aboutahir 1999; Bouabdellah et al. 2012). Specifically, these are (1) regionally extensive, pre-ore diagenetic replacement dolomitization that

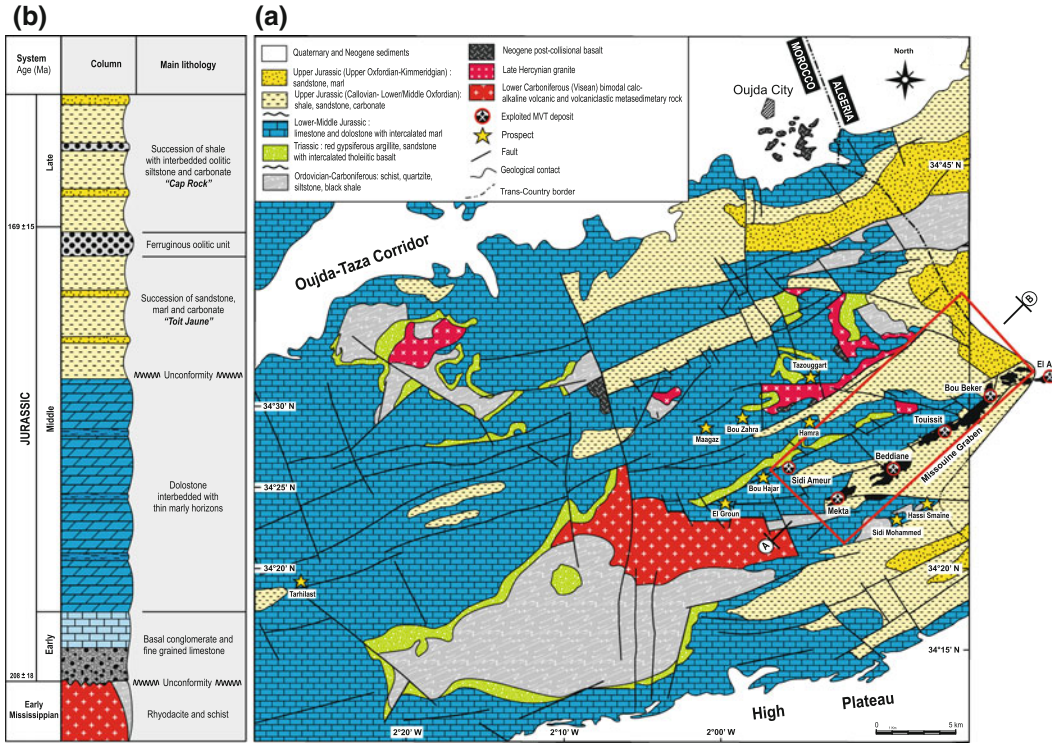

Fig. 4 **a** Geologic map of Touissit-Bou Beker district showing regional geology, major faults, distribution of ore-bearing dolostone, and associated MVT deposits (projected to surface). Regional geology simplified from Voirin (1965), Samson (1973), Owodenko (1976), Valin and Rakus (1979), and Bouabdellah et al. (2012, 2015). *Red rectangle* shows the location of the Touissit-Bou Beker district. **b** Generalized stratigraphic column for the Touissit-Bou Beker district showing main lithostratigraphic units. Section line *A–B* indicates cross-section presented in Fig. 5

forms 70 vol.% of the dolostone; and (2) epigenetic, ore-related, vug- and fracture-filling saddle dolomite cement.

The replacement dolomite pre-dates mineralization and significantly enhanced the porosity and permeability of the precursor limestones. In contrast, the ore-related hydrothermal sparry dolomite forms halos around the deposits and extends at least 100 m above the Aalenian-Bajocian dolostone host rocks into the overlying Upper Bajocian-Callovian-Oxfordian lithologies, and laterally for more than 10 km beyond the orebodies. Coexistence of the two types of dolomite led to the development diagnostic structures and textures that are commonly described in MVT environments elsewhere, such as saddle dolomite-cemented crackle, mosaic, and rubble breccias, and rock-matrix ("trash") breccias, zebra dolomite, and snow-on-roof texture (Bouabdellah et al. 2012).

Unlike dolomitization, silicification is weakly developed and is restricted to random, patchy-distributed occurrences of needle-like quartz crystals several centimetres long disseminated within the Aalenian-Bajocian dolostones.

2.4 Mineralization

The Pb–Zn deposits of the Touissit-Bou Beker district are epigenetic and stratabound. Sulphide mineralization consists principally of open-space fillings and metasomatic replacements of carbonate. Mineralization that fills open spaces (i.e.,

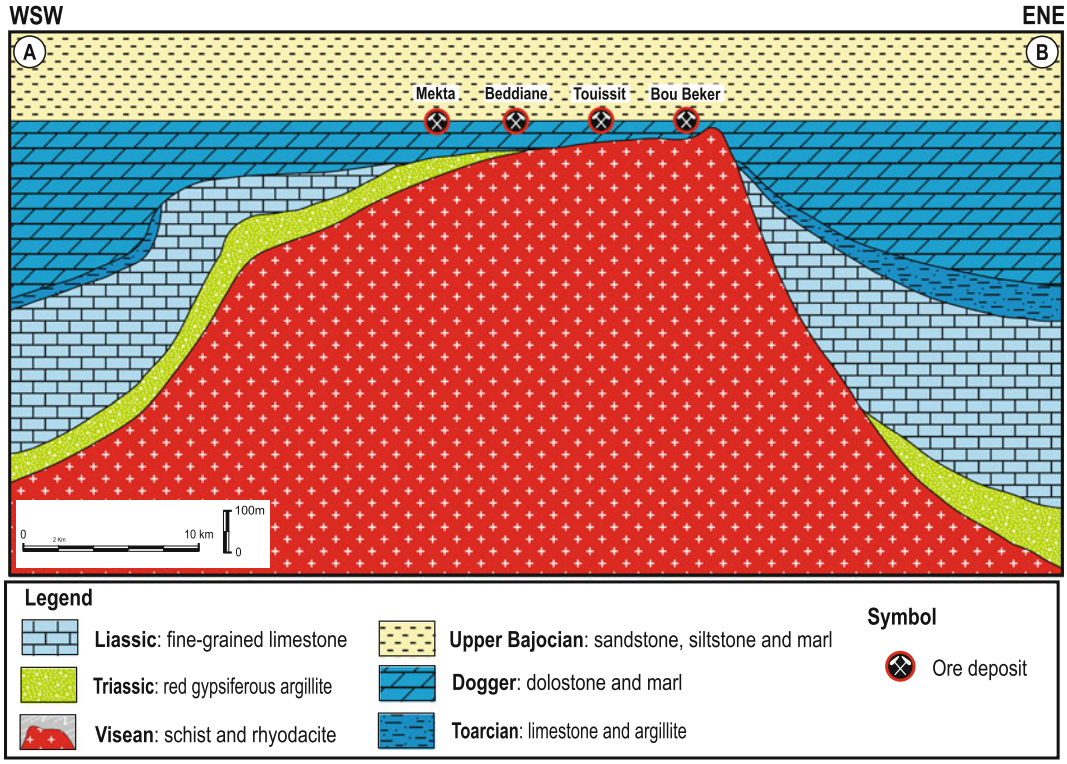

Fig. 5 Longitudinal ENE–WSW cross section through "Touissit Shelf" showing spatial distribution of main deposits of Touissit-Bou Beker district. Also illustrated is pinch-out of Triassic and overlying Liassic strata against "Touissit Shelf."

veins, interconnected cavities, or solution-collapse breccias) accounts for most of the high-grade orebodies (>80 % of extracted ore). These orebodies occur at various stratigraphic levels within the Aalenian-Bajocian (Middle Jurassic) strata, especially within the upper ten meters of the D_2 dolostone close to the upper Bajocian "Toit Jaune," and may extend for 10 m or more into the overlying Callovian-Oxfordian rocks (Fig. 4b). Uneconomic amounts of sulphides occur as veins (<1 m thick) within the Visean rhyodacitic basement. The mineralogy of the deposits is very simple, comprising sphalerite and galena, with minor pyrite-marcasite, and sparse chalcopyrite ± sulphosalts (i.e., tetrahedrite), accompanied by different generations of hydrothermal dolomite.

Field observations, together with mineralogical and textural relationships show that ore deposition occurred in three major stages, progressing from Zn-rich stage I to Pb-rich stage II and finally to a cuboctahedral stage III (Bouabdellah et al. 2012, 2015). Supergene mineral assemblages are extensively developed with oxidized ore zones extending as deep as 120 m, and account for nearly 60 % of the extracted ore. The transition from stage I to stage II mineralization is marked by the development of an intermediate Pb–Zn paragenesis in which mixed, co-genetic, fine-grained galena and sphalerite are intimately intergrown. Further evidence for the progressive evolution of the mineralizing fluid, from the Zn-rich to the Pb-rich ore stage, is shown by the presence of distinct metal zoning both vertically and laterally. Indeed, there is gradual decrease in Zn/Pb ratios from the east to the west and upward from the lower part to the uppermost part of the Aalenian-Bajocian dolomitic host rocks, with Zn/Pb ratios approaching unity in the case of

the Bou Beker and Touissit deposits (Bouabdellah et al. 2012).

The geometry of the orebodies that parallel the Atlasic ENE–WSW- and E–W-trending faults (Voirin 1965; Torbi and Gélard 1994; Jébrak et al. 1998) coupled with Pb–Pb geochronological data (Bouabdellah et al. 2012) suggest that the MVT mineralizing event occurred during the Miocene over a time span of <10 m.y., coincident with that recently proposed for the formation of carbonate-hosted Pb–Zn deposits in Tunisia (Jemmali et al. 2013).

2.5 Fluid Inclusion Thermometry

Microthermometric data performed on several generations of sphalerite and dolomite that span the paragenetic sequence (Dupy and Touray 1986; Makhoukhi et al. 2003; Aboutahir 1999; Bouabdellah et al. 2012) indicate that the ore-forming fluids correspond to evolved H_2O–NaCl–$CaCl_2$–KCl–$MgCl_2$ ± hydrocarbons hot (100 ± 20 °C) saline brines (>20 wt% NaCl equiv) of basin derivation. Calculated ore fluid pressures in the range of 150–200 bars (Makhoukhi et al. 2003) suggest depths of less than 1 km for ore deposition.

The high salinities and related high Ca/Na ratios of the ore-forming fluids imply that the predominant source of the ore-forming brine was seawater, although a contribution from halite dissolution to the total salt budget cannot be ruled out. Offset of fluid inclusion Na–Cl–Br leachate compositions away from the array for evaporated seawater was interpreted by Bouabdellah et al. (2012) to reflect dolomitization processes and fluid–rock interactions.

2.6 Stable Isotopes

Hundreds of carbon and oxygen isotope analyses were performed on several generations of replacement dolostones and ore-related hydrothermal dolomite cements (Bouabdellah 1994; Aboutahir 1999; Bouabdellah et al. 2012). Calculated $\delta^{18}O_{H2O}$ values of 3 ± 2 ‰ for the ore-forming fluids are consistent with several different sources, including connate waters, meteoric waters with long residence times in detrital rocks, and organically-derived (Sheppard 1986) and/or metamorphic waters. The absence of metamorphism of the Touissit-Bou Beker deposits excludes dehydration water as the ore fluid source. Organically-derived waters released from the organic-rich dolomitic host rocks and the unconformably overlying Bathonian black shales probably existed in the Touissit-Bou Beker deposits, but the low abundances of N_2, H_2S, and short-chain hydrocarbons within the fluid inclusions hosted in ore-related hydrothermal dolomite and sphalerite (Bouabdellah et al. 2012) suggest that organically-derived water was no more than a minor constituent. Furthermore, the high salinities of the fluid inclusions rule out meteoric water as the principal source of the ore-forming fluid, although meteoric water could have been a minor component. Alternatively, the Cl/Br and Na/Br molar ratios of the mineralizing fluids suggest that the source of the ore-forming brine was seawater that had evaporated beyond the point of halite saturation. Concurrently, the clustering of $\delta^{13}C$ values for all dolomite types at 0 ± 2 ‰, the typical value for Aalenian-Bajocian marine carbonate, implies that the dolomite carbon was inherited from the locally replaced limestone precursor.

In contrast to the uniform $\delta^{18}O$ and $\delta^{13}C$ values, sulphur isotope values for sulphide minerals display a wide range from −8.6 to + 12.9 ‰ (Bouabdellah et al. 2015). These values show distinct spatial (lateral and vertical) and temporal variations, expressed by an overall progressive decrease of $\delta^{34}S$ with (1) advancing paragenetic sequence toward younger sulfides (from stage I to stage III), (2) upward stratigraphic position (i.e., from base to top of the stratigraphic section), (3) towards the most distal parts of the deposits (i.e., surrounding prospects), and (4) within single grains (i.e., colloform-textured sphalerite) from the core toward the rim of analyzed sulphides. The resulting temporal shift from positive to negative $\delta^{34}S$ values may be interpreted as resulting from isotopic fractionation during inorganic (TSR) and/or bacteriogenic (BSR) reduction of seawater sulphate or porewater sulphate, at different rates of

sulphate availability (open versus closed reservoirs with respect to sulphate) (e.g., Basuki et al. 2008; Vikre et al. 2011). Mixing processes involving several sulphur sources having different $\delta^{34}S_{\Sigma S}$ values also can be invoked. Furthermore, the consistent decrease of $\delta^{34}S$ values both through space (i.e., towards higher stratigraphic position and more distal prospects) and time (i.e., with advancing paragenetic stage) is interpreted to reflect the entrainment of increasing amounts of surface fluid, possibly of meteoric origin, as this process would have resulted in oxidation of the fluids and shifting of $\delta^{34}S$ to lower values (Bouabdellah et al. 2015).

2.7 Radiogenic Isotopes

The $^{87}Sr/^{86}Sr$ ratios of replacement dolostones are similar to those of ore-related hydrothermal dolomites ranging from 0.70746 to 0.70833, and from 0.70769 to 0.70828, respectively, but are different from the ratios of the Visean rhyodacite (0.71849–0.72167) (Bouabdellah 1994; Bouabdellah et al. 2012). These $^{87}Sr/^{86}Sr$ ratios are higher than those for Aalenian-Bajocian seawater (0.70705–0.70735; Jenkyns et al. 2002). The negative correlation between $\delta^{18}O$ and $^{87}Sr/^{86}Sr$ isotopic ratios (Bouabdellah et al. 2012) suggests a link to deep circulation of the mineralizing fluids, probably at elevated temperatures, and as a consequence the input of radiogenic strontium from the underlying Visean rhyodacites, although the major source of dissolved strontium in the dolomitizing fluids was marine Aalenian-Bajocian carbonates.

Moreover, the lead isotope compositions of galena plot in a tight cluster above the evolution curve of Stacey and Kramers (1975), showing uniform $^{206}Pb/^{204}Pb$, $^{207}Pb/^{204}Pb$, and $^{208}Pb/^{204}Pb$ ratios ranging from 18.31 to 18.37, 15.61 to 15.66, and 38.45 to 38.62, respectively (Bouabdellah et al. 2012, 2015). Conversely, country rock samples display heterogeneous isotopic composition, with $^{206}Pb/^{204}Pb$ (17.76–18.49), $^{207}Pb/^{204}Pb$ (15.61–15.70), and $^{208}Pb/^{204}Pb$ (37.76–39.55) ratios defining two broad overlapping arrays on uranogenic and thorogenic plots (Bouabdellah et al. 2015). The tight linear clustering of Pb isotope data for galena from the ores, across the paragenetic sequence throughout the district, together with the overall tendency for the galena data to disperse along the Paleozoic, and more importantly the Mesozoic, sedimentary host-rock trends, led Bouabdellah et al. (2015) to conclude that Pb, and by inference other metals in the Touissit-Bou Beker district, were derived through the mixing of at least two main source-rock reservoirs characterized by contrasting Pb isotope compositions. The mineralizing process involved a large hydrothermal system that leached metals from the basement Visean rhyodacites and associated siliciclastic rocks, and more importantly from the overlying, multi-cycle, Triassic to Jurassic sediments including the "Toit Jaune" Pb-rich Bathonian sandstones.

2.8 Noble Gas Isotopes

Helium isotopic data for fluid inclusions show highly variable $^{3}He/^{4}He$ ratios ranging from completely radiogenic values of ~ 0.003 R_A to a maximum of 0.514 R_A (Bouabdellah et al. 2015). More interestingly, the distribution of $^{3}He/^{4}He$ ratios displays a distinct temporal and compositional trend including an overall decrease of $^{3}He/^{4}He$ ratios with advancing paragenetic sequence, consistent with the geochemical lowering trend exhibited by sulphur isotopic compositions. Overall, the highly variable $^{3}He/^{4}He$ ratios reflect variable degrees of mixing between mantle and crustal He along the flow path. The high concentration of ^{4}He, with a maximum of 38×10^{-8} cm^3/g (Bouabdellah et al. 2015), reflects prolonged residence times of the metalliferous brines within the basement host rocks prior to mineralization (Kendrick et al. 2002a, b). Long residence times of the resulting hot brines at such depths allowed them to equilibrate with the enclosing host rocks and attain high salinities, and as a consequence scavenge more metals.

Calculated contributions of the mantle-derived ^{4}He component involved in the paragenetically early Zn-rich, and succeeding Pb-rich main stages (i.e., $^{3}He/^{4}He$ ratios of ~ 0.15–0.51 R_A) are in the range of ~ 3–8 % for the

mineralizing fluids. This important finding led Bouabdellah et al. (2015) to conclude that the Late Neogene-Quaternary alkali basalts, which have ages coincident with the age of mineralization, could have contributed to the genesis of the Touissit-Bou Beker MVT mineralization by providing the necessary heat to drive fluid convection. The influence of mantle-derived He in the ore fluids decreased with time, consistent with the lowering of $\delta^{34}S$ values with advancing paragenetic sequence.

2.9 Ore Genesis

Conventional MVT genetic models including (1) episodic over-pressuring of compaction-driven fluids (Sharp 1978; Cathles and Smith 1983), (2) gravity-driven flow (e.g., Garven 1995; Bethke 1986), or (3) tectonically-driven "squeezing" flow (Oliver 1986) cannot satisfactorily account for Pb–Zn–Ag ore deposition in the Touissit-Bou Beker district (Bouabdellah et al. 2015). Of these, the widely accepted gravity-driven fluid model as a reliable driving force for fluid flow in this district may be possible (Bouabdellah et al. 2012), but seems unsupported by paleogeographic and paleoclimatic constraints. Indeed, this model assumes —even though not always clearly expressed—the existence of (1) a recharge zone that is permanently fueled by high rates of rainfall, and of (2) rapidly uplifted mountains as an efficient hydraulic head to create the high fluid flow velocities required to generate a fluid flow system efficient enough to form an economic deposit (Ge and Garven 1992; Appold and Garven 1999). However, paleogeographic and paleoclimatic reconstructions indicate that at the time of Pb–Zn mineralization in the Touissit-Bou Beker district (i.e., Late Neogene), Morocco and similarly the entire southwestern Mediterranean area, were under the influence of arid conditions (Fauquette et al. 2006). Moreover, structural data indicate that the later uplift stage, which took place during Messinian-Tortonian time (Frizon de Lamotte et al. 2009) contemporaneously with the emplacement of the Pb–Zn mineralization, did not exceed 1500 m. Based on these constraints, it is concluded that the gravity-driven fluid model would not have been efficienct enough to form ore deposits of the of sizes of those in the Touissit-Bou Beker district. An alternative model involving a genetic link among extensional tectonics, Neogene-Quaternary mafic magmatism, the Messinian salinity crisis, brine migration, and fluid mixing is therefore proposed for the Touissit-Bou Beker deposits (Bouabdellah et al. 2015).

The structurally controlled emplacement of the orebodies that parallel the Alpine ENE–WSW- and E–W-trending faults (Voirin 1965; Rajlich 1983; Torbi and Gélard 1994; Jébrak et al. 1998), coupled with lead isotopic constraints (Bouabdellah et al. 2012), suggest that the MVT mineralizing event occurred during the Miocene over a time span of 10 m.y. This inferred time period coincided with the emplacement of (1) Neogene to Quaternary calc-alkaline to alkaline basaltic magmatism (Duggen et al. 2005; Lustrino and Wilson 2007), and (2) a drastic paleoclimatic event at 5.96–5.33 Ma referred to as the Messinian salinity crisis (Hsü et al. 1973; Krijgsman et al. 1999). Indeed, the elevated $^{3}He/^{4}He$ ratios for fluid inclusions ($\sim$0.15–0.51 R_A; Bouabdellah et al. 2015) are consistent with the involvement of $\sim$3–8 % mantle-derived He, thus providing strong support for the contribution of mantle-derived volatiles and heat to the Touissit-Bou Beker mineralizing system. This addition of heat to the upper crust also may have promoted a long-lived convective hydrothermal system, consistent with the homogeneity of the galena Pb isotopic compositions and the formation of huge volumes of dolomitized rocks, which requires long-term fluid convection to provide a sufficient volume of dolomitizing fluids (Gomez-Rivas et al. 2014). The role of the Neogene-Quaternary basaltic magmatism was probably limited to providing the heat necessary to promote deep buoyancy driven, free convection and creating fluid conduits for focusing of the mineralizing hydrothermal brines into the permeable Aalenian-Bajocian ore-bearing dolostones.

The new model of Bouabdellah et al. (2015) also involves elevated heat flow and subsequent increased geothermal gradient initiated buoyancy-driven fluid convection of downward-flowing Messinian

seawater. This fluid convection ultimately promoted the mobilization of older, high-temperature, rock-buffered, dense brines stored within the Paleozoic basement, and the formation of base-metal-bearing chloride complexes. Mixing of Messinian seawater and basement-derived hydrothermal brines triggered the deposition of Pb- and Zn-rich stage I and II mineralization. The resulting mixed brines were mainly centered on the "Touissit Shelf" and its flanks, and then flowed laterally away from the basement high, giving rise to the lower grade mineralization of the distal prospects. The predominance of a high heat flow regime centered on a positive palaeographic structure (i.e., basement high) and more importantly the availability of appropriate sulphur nutrients (i.e., "fertile" vs. biogenic sulphur), may have been the critical ore controls that governed the size of the ore deposits.

3 Upper Moulouya District

The Upper Moulouya district of central Morocco (Fig. 6) constitutes the second largest producer of Pb in Morocco with a combined tonnage (production + reserves) of >31 Mt of ore at an average grade of ~4.5 wt% Pb (Annich and Rahhali 2002; Rahhali 2002). The mining district extends over a strike length of 40 km (east to west) and is 15 km wide (north to south), covering a total area of ~600 km^2. More than 100 Pb–Zn occurrences, ranging from small uneconomic showings to major deposits, have been delineated, three of which Aouli (9.6 Mt ore at 5 % Pb), Zeida (16 Mt at 3 % Pb), and Mibladen (6.5 Mt at 5 % Pb), are of economic interest (Fig. 7). Among these three deposits, only Mibladen is interpreted to belong to the MVT class (Jébrak et al. 1998; Naji 2004). At the present time, all of mines of the Upper Moulouya district are closed.

The village of Mibladen is famous as the source for most of the world's finest specimens of vanadinite (Jahn et al. 2003; Praszkier 2013). The Mibladen mining camp sensu stricto corresponds to an ENE-trending elongate area that extends for about 10 km (Fig. 8). Total production has been about 6.5 Mt of ore at 5 % Pb (Annich and Rahhali 2002; Rahhali 2002), accounting for approximately 30 % of Moroccan Pb production.

3.1 Mining History

Lead mining in the Upper Moulouya district has a long history with artisanal miners exploiting metals, particularly silver, since prehistoric and Medieval times (Emberger 1965). During the XII and the XIV Centuries, some deposits were mined by the Almohade Dynasty. In more recent times, mineral resources of the Mibladen area were re-discovered in the early 1920s and shortly thereafter were mined in open pits that produced lead concentrates. Between the 1920s and 1950s, mines of the district were owned and exploited by French mining companies, namely "la Société Penàrroya" and "la Société des Mines d'Aouli." The end of the 1950s and the beginning of 1960s marked the turning point in the district as an extensive exploration program was carried out to identify hidden deposits (Emberger 1965; Felenc and Lenoble 1965). Between 1968 and 1973, all of deposits were reevaluated during regional mapping (1:50,000 scale) and geochemical soil sampling, by a joint venture between the ONHYM "Office National des Hydrocarbures et des Mines" (formerly BRPM), the Ministry of Mines and Energy, and the Aouli Mining Company. The major period of lead mining ended with the closure in 1976 of the underground Mibladen mine.

3.2 District Geology Setting

The stratigraphy of the Upper Moulouya district consists of a succession of metamorphosed greenschist- to amphibolite-facies lower Paleozoic metasedimentary, volcaniclastic, and volcanic rocks, and unconformably overlying Mesozoic and Cenozoic strata (Emberger 1965; Fig. 6). The lower Paleozoic sequence comprises up to

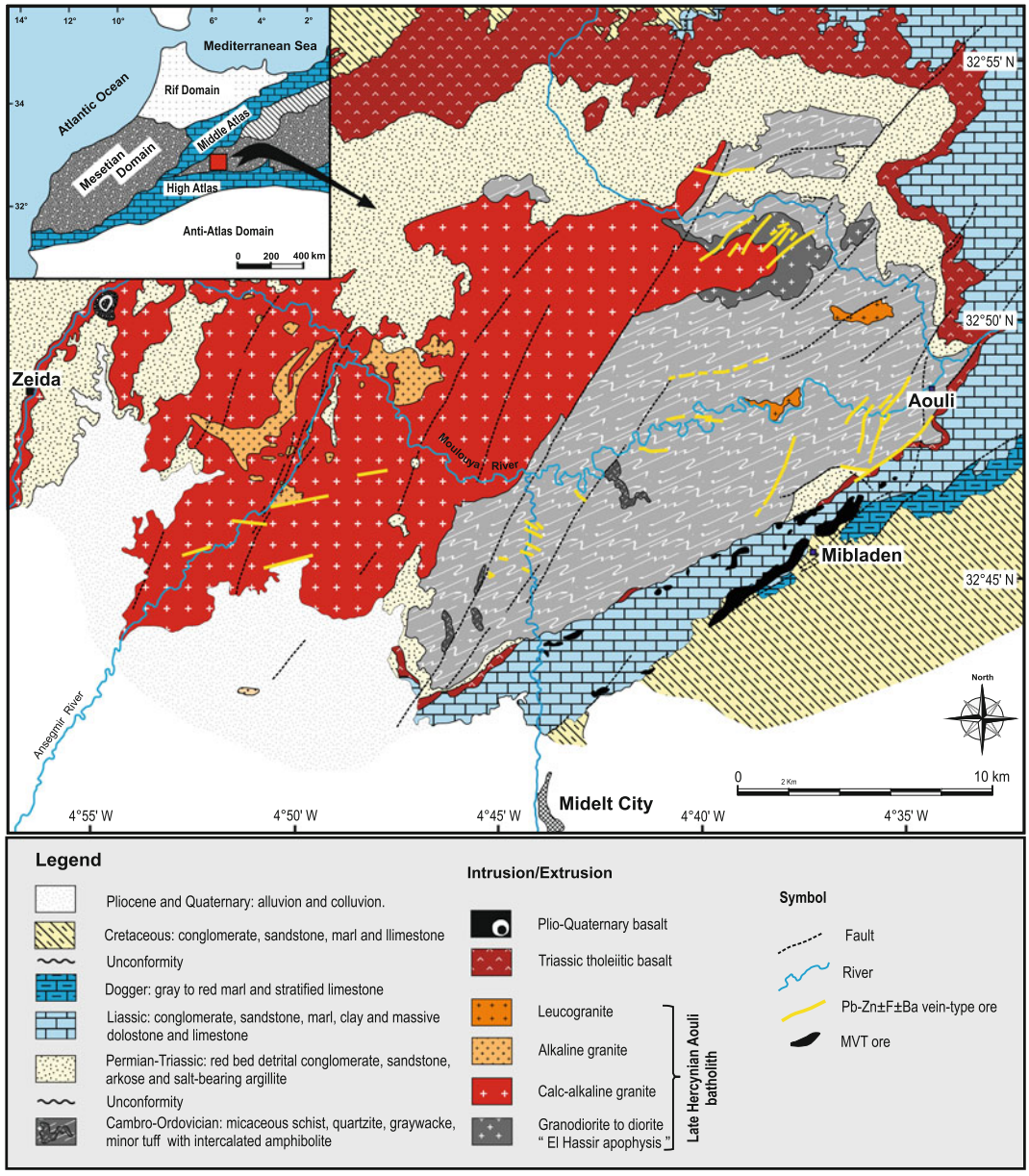

Fig. 6 Generalized geologic map of Upper Moulouya district showing regional geology, major faults, and location of historically mined Aouli, Mibladen, and Zeida base-metal ± fluorite ± barite deposits (modified after Emberger 1965). Inset shows Upper Moulouya district within framework of major tectonostratigraphic domains of northern Morocco

3,800 m of Cambro-Ordovician metasedimentary turbiditic flysch (Vauchez 1976; Filali et al. 1999) with intercalated mafic amphibolites. These rocks are locally intruded by the hydrothermally altered, multiphase, 347–281 ± 2 Ma alkaline to calc-alkaline Aouli granitoid batholith (Oukemini et al. 1995; Dahire 2004)

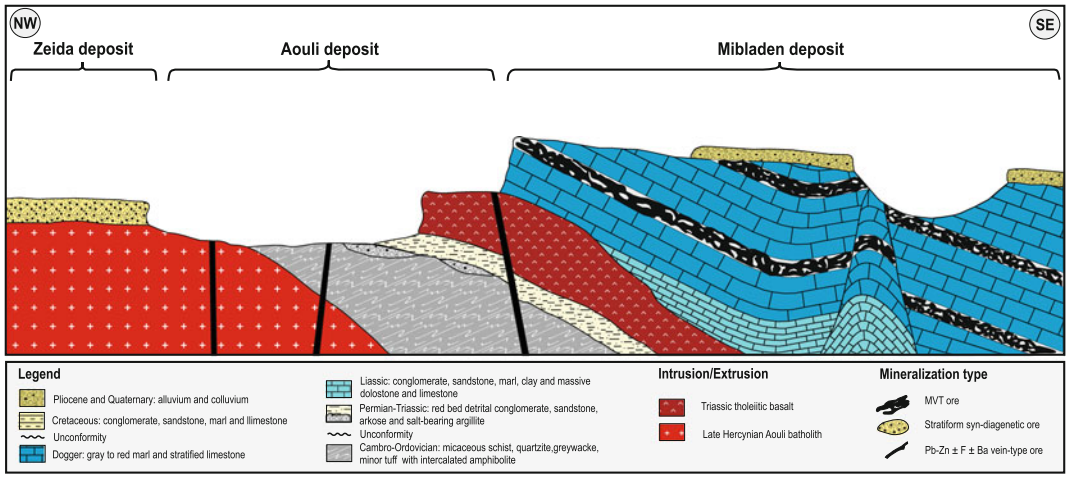

Fig. 7 Idealized longitudinal NW–SE cross section through Upper Moulouya district showing spatial distribution of Aouli, Zeida, and Mibladen base-metal ± fluorite ± barite deposits and their relationship to stratigraphy and fault systems (modified after Emberger 1965)

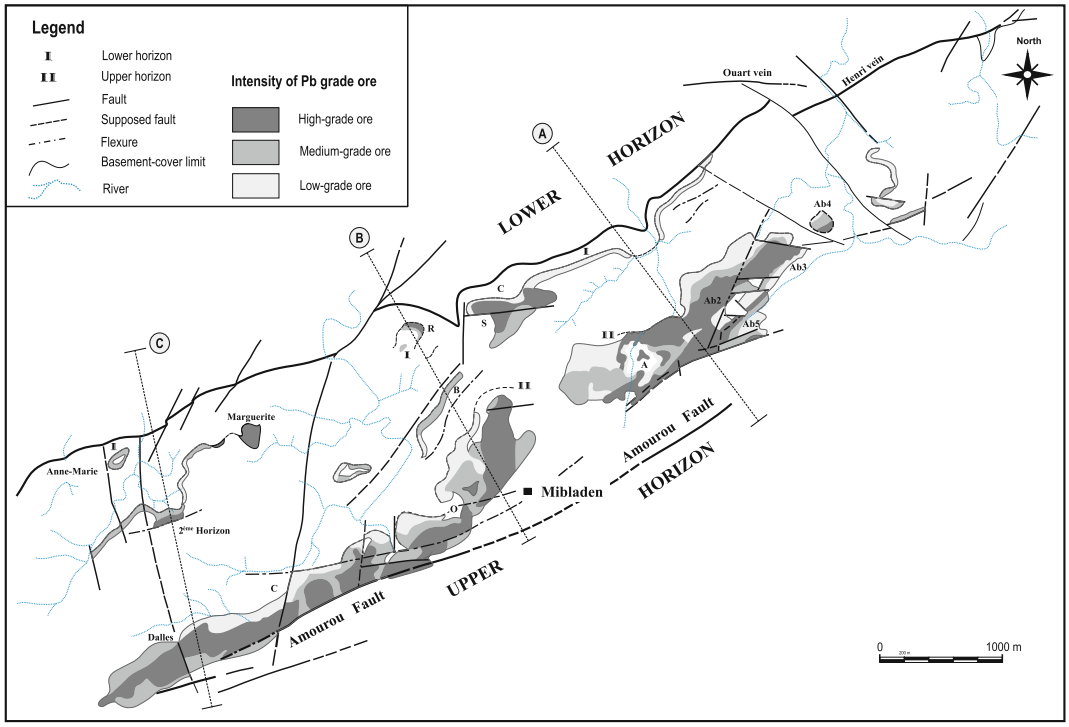

Fig. 8 Structural setting of Mibladen deposit with exploited MVT orebodies and contours of Pb grades projected to surface. Note that orebodies are elongate parallel to main fault system. Section lines *A*, *B*, and *C* refer to cross sections shown in Fig. 10. Modified from Felenc and Lenoble (1965)

From Triassic to Early Jurassic times the Upper Moulouya district experienced the influence of both the continental Atlantic and Tethys rifting processes (Ellouz et al. 2003; Ouarhache et al. 2012). This rifting resulted in the formation of syn- and post-rift, fault-controlled basins (i.e., horst and graben structures) that developed on a topographically high "shelf" during the major Triassic-Early Jurassic marine transgression (Ouarhache et al. 2012).

The syn-rift series consists of a thick (up to 1,000 m) succession of Permian to Triassic continental to fluvio-lacustrine red-bed sedimentary rocks with two main intercalated Central Atlantic Magmatic Province (CAMP) tholeiitic basaltic flows ca. 210 ± 2.1 to 196 ± 1.2 Ma ($^{40}Ar/^{39}Ar$; Fiechtner et al. 1992). The overlying, post-rift, Liassic to Dogger (Early-Middle Jurassic), shallow-water marine carbonates were deposited on a carbonate platform in a rapidly subsiding basin (Fedan et al. 1989). These strata are unconformably overlain by Cretaceous to Cenomanien shallow-marine carbonates, sandstones, marls, and shales, with intercalated units of lagoonar evaporites followed by up to 1,500 m of Miocene-Pliocene continental detrital sediments, locally intruded by ca. 14.6–0.5 Ma alkaline basaltic lava flows (Harmand and Cantagrel 1984; Duggen et al. 2009; Wittig et al. 2010).

It is noteworthy that the Domerian (Early Jurassic) dolomitized carbonates that host nearly all the economic occurrences of the Mibladen deposit experienced several episodes of karstification due to subaerial emergence of short duration in an active tensional tectonic regime (Dagallier and Macaudiere 1987). The Quaternary strata are made of alluvium and coluvium (Felenc and Lenoble 1965) and cap the lithostratigraphic column. Atlasic (Late Miocene) tectonic structures are dominated by a series of E–W-trending and subordinate ENE–WSW, NW–SE, and WNW–ESE kilometre-scale faults.

3.3 Alteration

Dolomitization and, to a lesser extent, silicification are the two main types of wall-rock alteration that affected the Domerian carbonate host rocks. Of these, the most pronounced alteration is expressed by regional, multi-stage, pre-ore and stratigraphically controlled diagenetic dolomite. Unlike this dolomitization, silicification is only weakly developed, being confined to centimeter-wide zones adjacent to the mineralized structures.

Pre-ore dolomitization forms massive replacements of the host rock carbonate but with most sedimentary fabrics such as bedding still preserved. This dolomitization prepared the host rocks for later MVT mineralization by increasing the initial porosity and permeability, and the competency of the precursor limestones. Unlike in the Touissit-Bou Beker district, ore-related hydrothermal dolomitization in the Upper Moulouya district is virtually absent.

3.4 Mineralization

The Mibladen Pb–Ba deposit extends over a wide stratigraphic interval within Triassic to Cretaceous strata. However, high-grade orebodies are exclusively confined to the Domerian (Early Jurassic) dolomitized carbonates. Mineralized structures are best developed in proximity to the major ENE-trending faults, namely the Aouli fault to the north and the Amourou fault to the south (Fig. 8). Overall, the sulphide-barite mineralization is clearly epigenetic and strata-bound, and occurs as massive fillings of horizontal and vertical karsts, veins, and of vuggy porosity related to dissolution of the host rocks infillings; to a lesser extent, this mineralization also forms metasomatic replacements (Fig. 9). The massive development of the orebodies within the upper 10 m of the Domerian

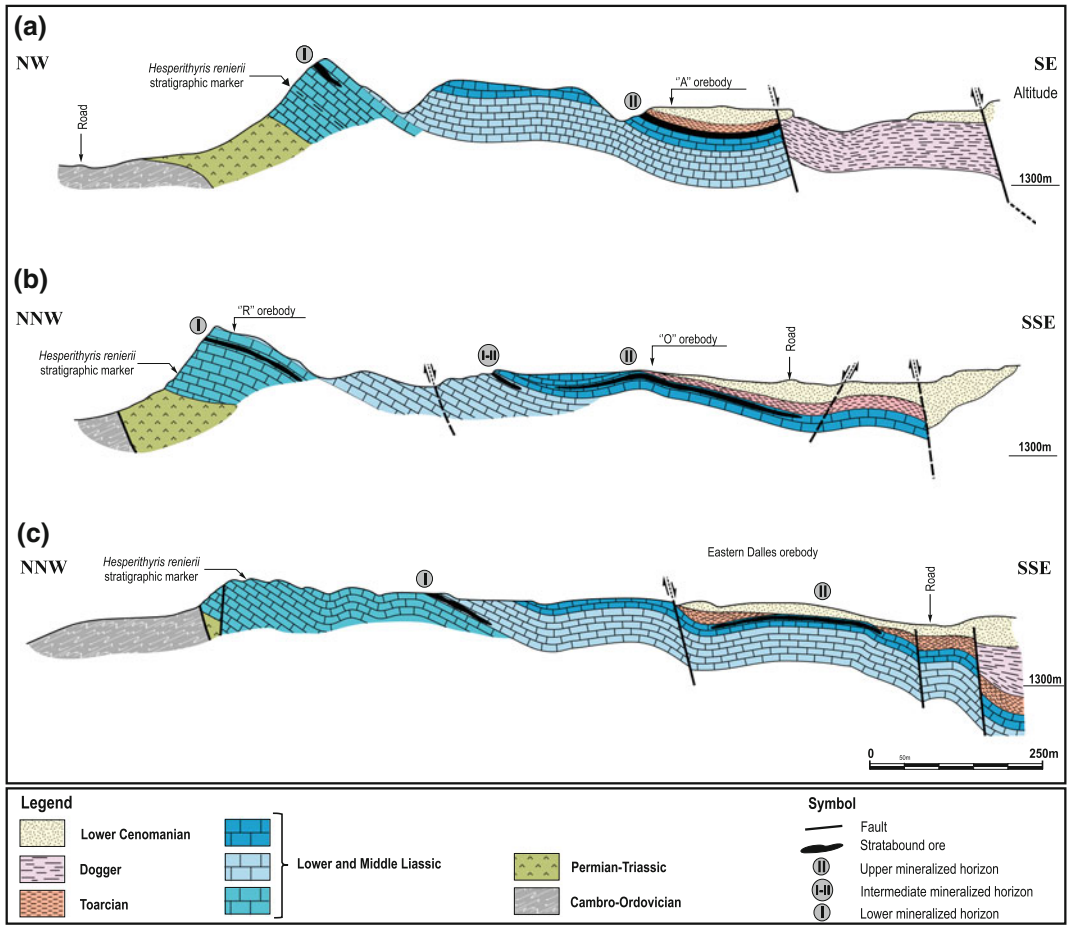

Fig. 9 Geological cross sections through Mibladen deposit in Upper Moulouya district illustrating morphology of MVT orebodies and post-Domerian age for mineralization. See Fig. 9 for locations of section lines. Modified after Agard and Du Dresnay (1965)

carbonates, near the Domerian-Toarcian unconformity, suggests that most of the dissolution structures, including early breccias and karst cavities, formed during periods of subaerial emergence. The higher grade, strata-bound orebodies are distributed along two main, sub-parallel, ENE-trending stratigraphic levels, locally referred to as upper and lower horizons (i.e., "Faisceau Supérieur" and "Faisceau inférieur," respectively; Felenc and Lenoble 1965) (Fig. 8).

Unlike the open-space filling galena that accounts for at least 90 % of the exploited ore, the metasomatic mineralization consists of less-economic, disseminated and/or grainy clusters of galena crystals that replace the dolomitized host rocks and associated sedimentary structures, giving rise to a stratiform style of mineralization.

3.5 Ore Mineralogy and Paragenesis

The mineralogy of the Mibladen deposit has among the simplest mineral assemblages ever documented for an MVT district. It consists mostly of galena, with minor amounts of pyrite and chalcopyrite. Sphalerite is virtually absent. Non-sulphide minerals are represented by barite with minor quartz. The unusual characteristic of

the Mibladen mineralogy results in the major predominance of lead over zinc with a Pb/Zn ratio of 10:1, and more importantly the development of an impressive supergene paragenesis from which some of the world's finest vanadinite, wulfenite, and cerussite specimens have been collected.

The sequence of mineral deposition shows three successive and overlapping stages of mineralization, two of which (Stages I and II) are of economic interest. Stage I, referred to as "main-stage ore," is the earliest and economically the most important, accounting for at least 80 vol.% of the total galena-barite resources. This stage comprises galena (Ga-1) and barite (Ba-1) accompanied by minor pyrite and chalcopyrite. Paragenetically later stage II mineralization, referred to as the "cuboctahedral stage," consists of centimeter-sized cubic to octahedral galena crystals (Ga-2) with white to pink crested barite (Ba-2) lining vugs.

Post-ore supergene Stage III resulting from the oxidation of hypogene sulphides consists of a rich secondary assemblage of vanadinite, wulfenite, cerussite, aragonite, calcite, quartz, gypsum, manganese oxides (coronadite, cryptomelane, and hollandite; Jahn et al. 2003), mottramite (PbCu$(VO_4)(OH)$), paralaurionite (PbCl(OH)), and phosgenite ($Pb_2CO_3Cl_2$) (Praszkier 2013).

3.6 Age of Mineralization

As debated for MVT deposits worldwide, the age of the Mibladen Pb mineralization has been, and still is, a source of ongoing controversy. Early debates focused on the question of whether the mineralization is syngenetic or epigenetic, and consequently occurred before or after the onset of the Atlasic orogeny in the Late Miocene. The lack of suitable minerals for radiometric dating along with the omnipresence of post-ore oxidizing events of unknown timing leave the age of hypogene mineralization uncertain.

Combined geological field observations and cross-cutting relationships have been used to estimate the relative timing of mineralization. Paragenetic studies show the presence of two distinct stages of mineralization, both of which are epigenetic and structurally controlled and formed after lithification and dissolution of the Domerian dolomitic host rocks. Thus, the deposition of these two stages post-dates the Early Jurassic (i.e., Domerian). More importantly, the $\delta^{34}S$ values of barite range from 17.1 to 18.1 ‰ (Table 1) and plot within the compositional interval for Cretaceous seawater, with an average range of 15–20 ‰ (Claypool et al. 1980; Kampschulte and Strauss 2004). These sulphur isotope data suggest that sulphur in the barite was derived from coeval seawater sulphate, either directly from the Cretaceous ocean or by the dissolution of Cretaceous marine evaporates. If so, this would place a maximum age of ~100 Ma for the Pb mineralization. However, based on the fault geometry and siting of economic orebodies within the Mibladen deposit, it is inferred that the ENE-, E–W-, and NW-trending fault zones acted as major fluid conduits for MVT mineralizing fluids. These fault systems are interpreted to have been reactivated during Neogene time, by tectonic inversion of preexisting Jurassic normal faults in response to NW–SE- and N–S-directed compressional events (Naji 2004).

Based on these constraints and the strong similarities in mineral assemblages and the nature and conditions of the mineralizing fluids with the Touissit-Bou Beker mineralization described above, it is concluded that the Mibladen MVT mineralization formed during the Late Miocene during the same time period in which the Touissit-Bou Beker mineralization formed. The same arguments and conclusions were reached previously by Jébrak et al. (1998).

3.7 Fluid Inclusion Microthermometry

At the Mibladen deposit, the only suitable mineral for fluid inclusions studies is barite. However, this is a questionable host mineral for microthermometric measurements due to its soft nature and tendency to stretch or leak during heating (e.g., Ulrich and Bodnar 1988).

Table 1 Sulphur and lead isotopic compositions of galena and barite separates from Mibladen (Upper Moulouya) and Jbel Bou Dahar (Eastern High Atlas) MVT deposits

Deposit/District	Mineral separate	$\delta^{34}S$	$^{206}Pb/^{204}Pb$	$^{208}Pb/^{204}Pb$
Mibladen	Galena	−20.5	18.268	38.484
Mibladen	Galena	−22.2	–	–
Mibladen	Galena	−19.7	–	–
Mibladen	Galena	−24.6	–	–
Mibladen	Galena	−21.9	–	–
Mibladen	Galena	−24.6	–	–
Mibladen	Galena	−23.2	18.250	38.413
Mibladen	Galena	−22.1	–	–
Mibladen	Galena	−23.4	–	–
Mibladen	Galena	−23.3	18.282	38.548
Mibladen	Barite	17.7	–	–
Mibladen	Barite	17.9	–	–
Mibladen	Barite	17.1	–	–
Mibladen	Barite	16.8	–	–
Mibladen	Barite	16.8	–	–
Mibladen	Barite	16.3	–	–
Mibladen	Barite	18.1	–	–
Jbel Bou Dahar	Galena	–	18.205	38.376
Jbel Bou Dahar	Galena	–	18.189	38.442
Jbel Bou Dahar	Galena	–	18.191	38.378
Jbel Bou Dahar	Galena	–	18.111	38.380

However, Kontak and Sangster (2005) challenged this statement and noted that, by careful examination, reliable fluid inclusion data can be extracted from barite. Being aware of such constraints, we carried out a series of microthermometric measurements on selected barite samples. The two-phase aqueous inclusions were overheated by up to 100 °C and then the T_h value was remeasured. Statistical treatment of the obtained data was applied and all of the abnormal temperatures (not on a Gaussian curve) were therefore not used. Accordingly, we think that the wide ranges of homogenization temperatures may be considered reliable and not related to stretching phenomena.

Altogether, the measured T_h values display homogenization temperatures of ~120°–~190 °C and salinities of ca. 14–24 wt% NaCl equiv (Table 2; Fig. 10). These wide ranges in both temperature and salinity fall within the ranges for present-day oil-field brines and ancient Mississippi Valley-type mineralizing fluids (Carpenter et al. 1974; Haynes and Kesler 1987; Leach and Sangster 1993), and are similar to the values obtained for MVT deposits worldwide (Leach et al. 2010; and references herein).

3.8 Sulphur and Lead Isotopes

Sulphur isotope compositions for galena separates that span the main stages of ore mineralization are all negative with $\delta^{34}S$ values of −24.6 ‰ to −19.7 (mean = −22.5, σ = 1.6 ‰; n = 10; Table 1). These sulphur isotopic compositions are among the lightest $\delta^{34}S$ values ever recorded for North African MVTs, and are similar to those reported for the Austrian MVT deposits in Bleiberg (Kucha et al. 2010). Overall, these $\delta^{34}S$ values are substantially lower than the range of $\delta^{34}S$ that characterizes Jurassic-Cretaceous seawater sulphate (~10–23 ‰; Claypool et al. 1980; Kampschulte

Table 2 Summary of microthermometric data (homogenization temperatures and salinities) for fluid inclusions in barite from Mibladen deposit in the Upper Moulouya district

Mineral	T_e					$T_{m(ice)}$					T_h					Salinity				
	n	Min	Max	Avg.	Std. Dev	n	Min	Max	Avg.	Std. Dev	n	Min	Max	Avg.	Std. Dev	n	Min	Max	Avg.	Std. Dev
Barite	38	−80	−45	−61	9	34	−21	−10	−14	3	51	122	199	170	20	34	14	23	18	2

Abbreviation: *Avg.* average; *n* number of measurements; *Max* maximum; *Min* minimum; *Std. Dev* standard deviation

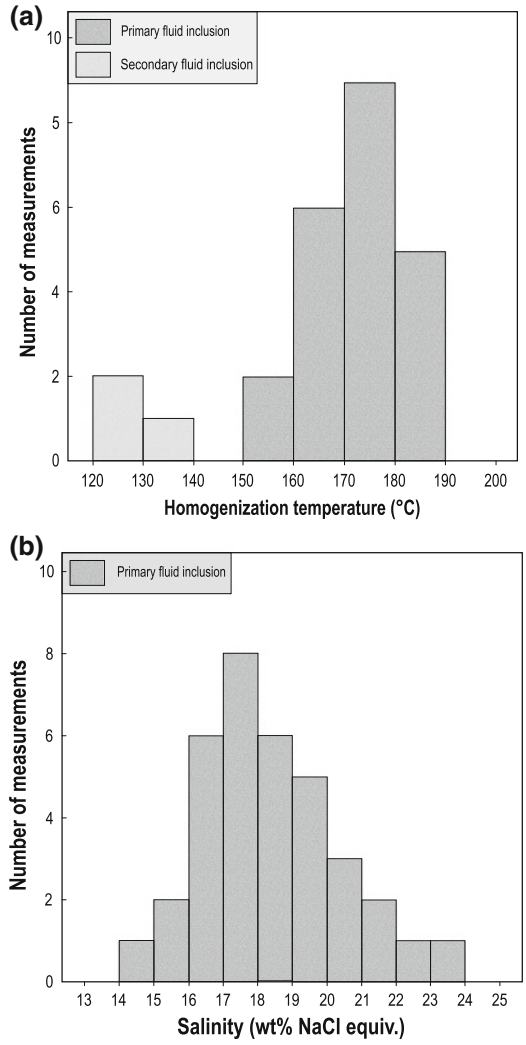

Fig. 10 Histograms of salinity (**a**) and homogenization temperature (**b**) for fluid inclusions in barite from Mibladen deposit in Upper Moulouya district

and Strauss 2004). Conversely, the sulphur isotope compositions of the paragenetically late barite, which range from 16.3 to 18.1 ‰ (mean = 17.2, σ = 0.7 ‰, n = 7; Table 1), are similar to Cretaceous seawater sulphate values (~10–22 ‰; Claypool et al. 1980; Kampschulte and Strauss 2004). This comparison suggests that sulphur in the barite was derived from coeval seawater sulphate either directly from the Cretaceous ocean or from dissolved marine evaporates. The underlying Triassic evaporates that potentially could have acted as the source of sulphur are not considered here because of the discrepancy between the sulphur isotopic compositions of these evaporates (mean $\delta^{34}S$ 13.7 ± 0.7 ‰; Bouabdellah et al. 2012) and values recorded for the barite (i.e., mean $\delta^{34}S$ 17.2 ± 0.7 ‰).

The strongly negative $\delta^{34}S$ values that characterize the Mibladen galena ore are indicative of bacteriogenic reduction of seawater sulphate (BSR) or of pore seawater in a system open to sulphate (e.g., Basuki et al. 2008; Vikre et al. 2011). Calculated $\Delta_{SO4\text{-galena}}$ values that are significantly greater than 20 ‰ exclude thermochemical sulphate reduction (TSR) as the main ore depositional process, thus leaving BSR as the most viable process responsible for the extremely low $\delta^{34}S$ values. Oil-window thermal maturation and degradation of organic matter dispersed within the Jurassic carbonates could have played a direct role in BSR and/or acted indirectly as a reductant for sulphate by releasing the H_2S component required for metal precipitation. Bacterial activity therefore may have been fed by hydrocarbon brines and sulphate remobilized from Cretaceous evaporites. The very low $\delta^{34}S$ values could also reflect reduced sulphur derived from diagenetic framboidal pyrite contained within the Jurassic sedimentary succession. However, the very low abundance of pyrite in the host strata of the Mibladen area makes this possibility unlikely.

Conversely, lead isotopic compositions of galena separates from the Mibladen deposit plot in a tight cluster above the evolution curve of Stacey and Kramers (1975) and show relatively uniform $^{206}Pb/^{204}Pb$, $^{207}Pb/^{204}Pb$, and $^{208}Pb/^{204}Pb$ ratios from 18.250 to 18.282, 15.607 to 15.645, and 38.413 to 38.548; respectively (Fig. 11). These isotopic compositions are roughly consistent with the range of Pb-isotopic ratios presented by Duthou et al. (1976) and Jébrak et al. (1998). Moreover, similarity in lead isotopic compositions for K-feldspar mineral separates from the Aouli intrusion (Jébrak et al. 1998) and the galena ore strongly suggest that the

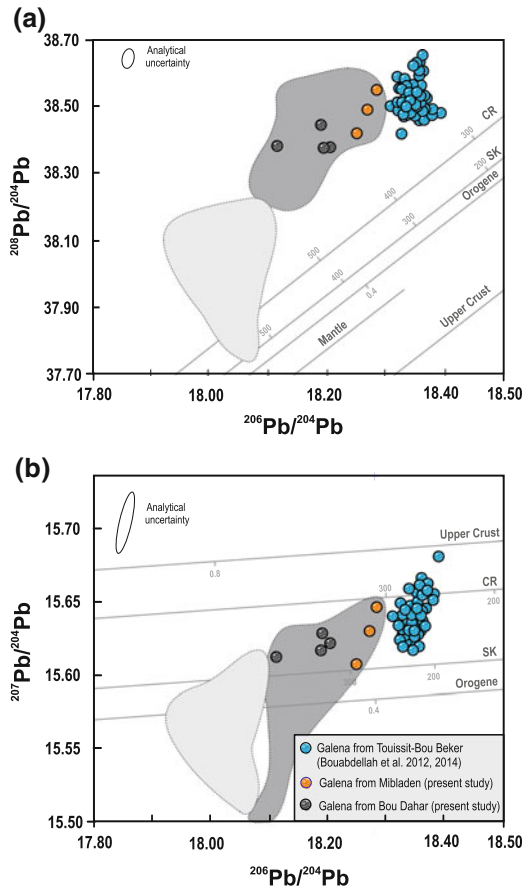

Fig. 11 Lead isotopic compositions of galena separates from Mibladen and Jbel Bou Dahar MVT districts compared to those from Touissit-Bou Beker district (Bouabdellah et al. 2015). **a** $^{208}Pb/^{204}Pb$ versus $^{206}Pb/^{204}Pb$; **b** $^{207}Pb/^{204}Pb$ versus $^{206}Pb/^{204}Pb$. Evolution curves of Stacey and Kramers (1975) and Cumming and Richards (1975) are labeled S and K and C and R, respectively; evolution curves for Upper Crust and Orogene (Zartman and Doe 1981) are shown for reference. Dark grey field defines galena isotopic compositions for Aouli-Mibladen district. Light grey field shows range of K-feldspar lead isotopic compositions for Late Hercynian granite from the Upper Moulouya district (Vitrac et al. 1981; Jébrak et al. 1998)

Late Hercynian granitoids were the main lead source, involving the leaching of K-feldspars, with possibly minor amounts of lead being derived from the Triassic arkoses. Compared to the ore lead isotope data for Touissit-Bou Beker, the Mibladen galena separates exhibit less radiogenic compositions (Fig. 11).

3.9 Proposed Genetic Model

Because no radiometric age for the emplacement of the Mibladen mineralization is available, the following proposed genetic model is only a first attempt toward the development of a more robust model.

Combining field relationships together with the petrographic and geochemical data presented above, it appears that the Mibladen MVT orebodies formed in mid-Tertiary time in response to large-scale crustal processes triggered by the Atlasic orogeny. Moreover, the fact that economic MVT mineralization is restricted to the Domerian carbonates strongly suggests that this formation constituted the main regional aquifer for the Mibladen mineralizing brines.

In addition to stratigraphy, the main ore controls include paleogeography (i.e., basement high and associated sedimentary pinchouts), brecciation and karstification (i.e., cavity filling mineralization), alteration (i.e., extensive dolomitization with subordinate silicification), and more importantly faulting. Indeed, the intimate relationship between the ENE- and WNW-trending faults and orebodies provides strong evidence that these faults were the major pathways that focused fluid flow. Compared to the Touissit-Bou Beker district, the Mibladen mineralization shares many empirical attributes that are common to the two districts. There are, however, a few differences that set the Mibladen district apart. These include (1) occurrence of barite as the principal gangue mineral rather than saddle dolomite, and (2) very high Pb/Zn ratios with sphalerite being virtually absent.

Data for fluid inclusions together with sulphur and lead isotopes indicate that the ore fluids were moderately hot (>100 °C) basin-derived brines that scavenged lead and associated metals from the underlying Late Hercynian granitoids and their overlying clastic rock derivates. The large quantities of both barite and the very low-$\delta^{34}S_{sulphide}$ values in the Mibladen deposit suggest, as also proposed by Hitzman and Beaty (1996) for the Irish deposits, a continuous resupply of marine sulphate and bacteriogenetically reduced sulphide to the site of

mineralization. This model indicates that there must have been communication with either a large reservoir of sulphate-rich formation water or with the Jurassic-Cretaceous Ocean.

The wide discrepancy between $\delta^{34}S$ values of galena and barite rules out the single model as the possible depositional mechanism for the Mibladen deposit. Instead, these data point to fluid mixing of at least two incompatible fluid reservoirs, as also suggested by coexistence of intergrown sulphides and barite. Similarly, the negative correlation between sulphur and lead isotope compositions (Jébrak et al. 1998) is interpreted to represent fluid mixing between two end-members: (1) a deep-seated, basement-equilibrated hydrothermal fluid; and (2) a surficial formation and/or meteoric water. The absence of extensive silicification in the wall rocks, which may reflect suppression of silica saturation by fluid mixing and dilution (Plumlee et al. 1994), coupled with the lack of evidence for fluid immiscibility indicates that an abrupt temperature decrease did not occur during fluid mixing. Moreover, the development of pervasive dissolution and replacement textures indicates acidic fluid conditions. This scenario requires a second depositional mechanism. Indeed, neutralization of the deep-seated fluid by reaction with the Domerian carbonate host rocks would have decreased metal solubilities, ultimately leading to development of the replacement-style mineralization. The reduced sulphur required for precipitation of the sulphides derived principally by BSR of aqueous sulphate. During the subsequent deposition of late barite, the oxidation state of the mineralizing fluid must have shifted towards more oxidizing conditions.

In order to maintain an efficient downward deep circulation of the mineralizing fluids, an uplift episode is required to provide the necessary hydrologic head for fluid movement. As mineralization is inferred to have occurred during Mid-Tertiary time that coincides with major uplift of the Atlas belt, we propose a gravity-driven flow model in which fluids recharged in the Atlas migrated through the Domerian aquifer along deep-seated ENE-trending faults. This fluid migration thereby drove the high salinity, mineralizing brines toward the edges of the basin where deposition of sulphides occurred, by fluid mixing with sulphur derived by BSR. In our model, downward-flowing and oxidized, SO_4^{2-} and Cl^--rich ground waters mixed with the deeper reduced H_2S-rich saline waters to form H_2SO_4. Barite precipitated where Ba^{2+} in the reduced fluid reacted with SO_4^{2-} that was generated in the mixing zone, thus explaining the abundance of barite in the late stages of ore formation.

4 Jbel Bou Dahar District

The Jbel Bou Dahar plateau (32°18′0″ N, 3°18′0′′ E) is located within the eastern part of the High Atlas Mountains. More than 20 economic Pb–Zn prospects and deposits are distributed along the margins of the Lower Jurassic reef carbonate platform, particularly its southern flank (Fig. 12). From 1961 to 1965, the district has produced about 100,000 t of Pb and 20,000 t of Zn (Agard et Du Dresnay 1965). At the present time, widespread exploration continues in the district focusing on productive targets.

4.1 District Geology

The present-day high-relief Jbel Bou Dahar plateau forms an elongate, ENE-trending, reefal structure 40 km × 15 km in size that encompasses a total area of ~600 km^2 (Fig. 12). The geologic setting of this plateau has been described in numerous papers (Agard and Dresnay Du 1965; Dresnay Du 1979; Evans and Kendall 1977; Warme 1988; Crevello 1990; Kenter and Campbell 1991; Blomeier and Reijmer 2002; Merino-Tomé et al. 2012; Rddad and Bouhlel 2016), from which the following summary has been inspired.

The core of the carbonate platform, which is exposed in the northern part of the reefal structure (i.e., Sebbab-Kébir inlier, Fig. 12), consists of a succession of greenschist-facies Cambro-Ordovician to Silurian metasedimentary and volcaniclastic rocks made dominantly of quartzite and schist. Unconformably overlying the

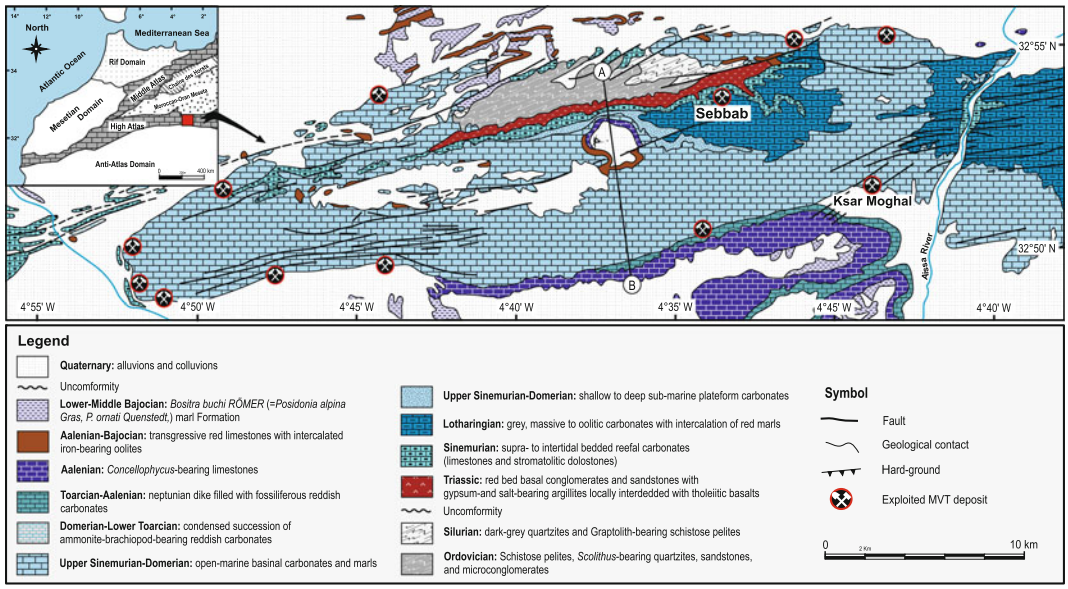

Fig. 12 Geological map of Jbel Bou Dahar early Mesozoic annular reefal complex emphasizing regional geology, main tectonic structures, and stratigraphic distribution of major MVT deposits. Line *A*–*B* indicates cross section shown in Fig. 13. Modified after Agard and Du Dresnay (1965)

metasedimentary Paleozoic package is a ~400–500 m sequence of Triassic sedimentary rocks consisting of red-bed siltstone and gypsiferous to salt-bearing argillite locally interbedded with CAMP tholeiitic basalts. During Early and Middle Liassic times, the lower Paleozoic formed a topographic high on which the Jbel Bou Dahar reef and lagoon were built, incompletely separated from the open sea by a barrier reef that developed to the south (Fig. 13). Strata of the Jbel Bou Dahar reef undergo a series of facies changes from an offshore basinal shale and limestone facies, through the undolomitized reef, to a back-reef facies having abundant porosity.

The reef deposits consist of unmetamorphosed, massive, coral-algal- and bivalve-bearing Pleinsbachian, flat-lying, thickly-bedded carbonate mudstone, skeletal wackestone, skeletal pelletal packstone, laminated carbonate mudstone, and calcareous clay. The sequence attains a maximum thickness of 175 m at the axis of the barrier and thins both south and north, forming a lens-like bank of sediment. Platform growth was initiated during the Sinemurian and ended at the Domerian (Upper Pliensbachian) and the Middle Toarcian (Crevello 1990; Blomeier and Reumer 1999). Toarcian shales and Aalenian lime mudstones progressively onlap the flanks of the Domerian platform and conformably overly the platform roof, recording an abrupt cessation of platform evolution at the Domerian-Toarcian transition (Crevello 1990; Campbell and Stafleu 1992). Dolomitization is restricted to the Sinemurian carbonates and is not observed in the Domerian rocks. During the Bajocian, the basin filled completely and became a continentally emergent structure by the Late Bajocian, or certainly by the Bathonian (Dresnay Du 1979).

The deformational history of the Jbel Bou Dahar plateau is divided into Hercynian (late Paleozoic) and Atlasic (Mesozoic to Tertiary) cycles. The predominant Atlasic fault structures form a consistent array, with many trending ENE–WSW, some larger and more continuous faults trending E–W, and a subsidiary set trending NNW–SSE. ENE- and E–W-trending faults probably played an important role in focusing the flow of ore-forming fluids, as suggested by

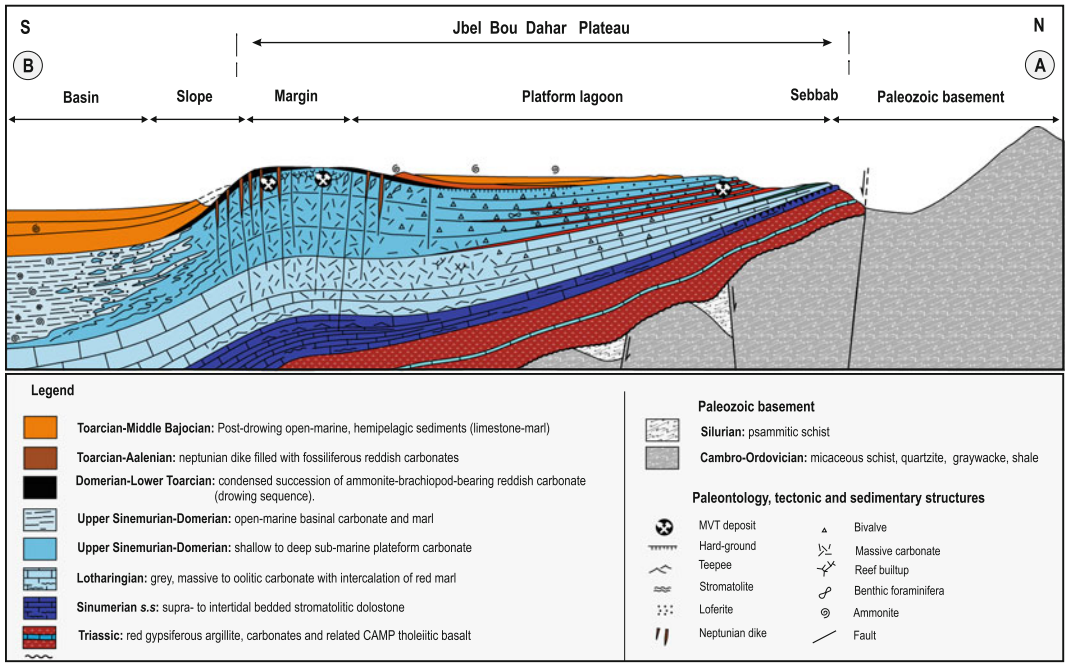

Fig. 13 N–S geological section along strike of Jbel Bou Dahar early Mesozoic carbonate platform showing spatial distribution of main lithofacies associations and MVT deposits; see Fig. 13 for location of section. Modified after Agard and Du Dresnay (1965)

proximity of these faults to the orebodies and by the general elongation of mineralized veins and ore zones in ENE and E–W directions (Fig. 12).

4.2 Alteration

The main wall-rock alteration in the Jbel Bou Dahar district is confined to patchy silicification and minor dolomitization. Although silicification could be interpreted as resulting from diagenetic alteration (Scheibner and Reumer 1999), the proximal location of the quartz alteration halo to the wall rocks of the mineralized structures suggests that this silicification is probably related to hydrothermal activity, and not to diagenesis. Dolomitization is weak or nonexistent. Unlike in the Touissit-Bou Beker and Upper Moulouya districts described above, neither pre-ore replacement nor ore-related hydrothermal dolomitization affected the Pliensbachian carbonate host rocks.

The most diagnostic feature of wall-rock alteration in the Jbel Bou Dahar district is intense veining and open-space filling by sparry calcite ± barite ± celestine typically developed immediately adjacent to the Pb–Zn orebodies. The white sparry calcite occurs as pre-, syn-, and post-ore massive fillings of veins, veinlets, karst cavities and related crackle and dissolution collapse-breccias, and echelon tension gashes intimately related to Pb–Zn mineralization. Of historical note, this sparry calcite was used by indigenous prospectors as a reliable guide to hidden Pb–Zn showings.

4.3 Mineralization

The district sulphide ± barite ± celestite deposits consist principally of galena and sphalerite with subordinate pyrite/marcasite and chalcopyrite. This mineralization is clearly epigenetic and predominantly stratabound, although local stratiform mineralization is also economically important (i.e., Sebbab deposit; Fig. 12). Economic sulphide mineralization may occur throughout all

the lithostratigraphic units, it is typically confined to the reef facies and/or to pinchouts of the Liassic strata against Paleozoic basement high (Fig. 13). Therefore, prominent ore controls are related to depositional pinchouts and configuration of the basement surface (i.e., presence of paleohigh structures).

Based on stratigraphic position, geometry of ore occurrences, and nature of the Pb–Zn deposits, two main styles of mineralization are distinguished: (1) open-space fillings, and (2) metasomatic replacements. Economic orebodies occur at various stratigraphic levels within the Lower to Middle Jurassic strata, from the Lotharingian to the Aalenian, with most of the higher-grade orebodies confined to the brecciated, Pliensbachian coarse sand to gravel, bioclastic bivalve-coral-algal packstones. Uneconomic mineralization that forms thin centimeter-thick veins may extend into the underlying Cambro-Ordovician schistose basement rocks.

Replacement mineralization occurs more commonly as interstitial sulphide disseminations of variable size and to a lesser extent as tabular lenses in which ore textures obliterate original sedimentary textures of the replaced Lotharingian oolitic reefal limestones and associated sub-reefal brecciated carbonates. Geometry of the sulphide masses appears to have been controlled by preferential replacement of specific carbonate units (i.e., bedded ooid, intraclast, and pisoid packstones to rudstones), and along stratigraphic contacts. The most representative example of this type of mineralization is shown by the Sebbab deposit (Fig. 12) and a large number of prospects exposed along the southern flank of the Jbel Bou Dahar reefal complex, where extensive and pervasive replacement of the carbonate host rocks is expressed by pseudomorphic remnants of bioclasts and faunal assemblages (Adil 2004).

At the Sebbab deposit, sulphide mineralization is distributed along two main, sub-parallel, ENE-trending levels, referred to as upper and lower horizons. These delineated mineralized zones, defined on the basis of the ~2 % Pb contour, follow the trend of the main extensional faults and are separated by undisturbed, massive, impermeable red marls. Irrespective of mineralized zone, Sebbab mineralization is characterized by fine-grained ore and locally the presence of dendritic sulphides.

Higher grade orebodies, accounting for more than 90 % of the extracted ore in the district, occur as massive fillings of fractures, veinlets, veins, karsts, and a variety of vuggy pore spaces, and as cements in solution collapse breccias related to post-lithification dissolution of brecciated Pliensbachian reefal carbonates. Locally, sulphide mineralization fills and cuts compactional stylolites. There is clear evidence that open-space deposition was accompanied by extensive dissolution and replacement of the Lower Jurassic carbonates.

Vein-type mineralization shows various morphologies ranging from planar centimeter- to kilometer-scale veins and veinlets, boudinage, and "en echelon" to sigmoidal arrays. Economic orebodies are confined to calcite-sulphide-barite veins localized along the intersection of E–W- and NE-trending fault arrays (i.e., "noeud tectoniques"). The most important of the structurally controlled veins is represented by the Ksar Moghal deposit (Fig. 12), from which 80,000 t of Pb concentrates have been produced (Agard and Du Dresnay 1965). In this deposit, two main vein sets, including the multi-kilometer, ENE-striking vein system and the E–W-trending vein array, are by far the dominant mineralizing structures. The exploited structures can be more than 1 km long, up to 4 m wide, and are mainly filled with galena, and form sub-vertical, WNW–ESE-striking brecciated major faults that dip steeply to the south and have vertical extents exceeding 150 m, without significant change in mineral assemblage.

4.4 Ore Mineralogy, Textures, and Paragenesis

The ore mineralogy is fairly simple and consists of variable amounts of sphalerite, galena, pyrite-marcasite, and chalcopyrite, accompanied by barite, celestite, and calcite as the main

gangue minerals. Sphalerite and galena are intimately intergrown, but display unequal proportions from deposit to deposit, and even within a single orebody. Common MVT ore textures include crackle breccias, collapse breccias, and impregnations.

The near surface of the exploited open pits and underground exposures contain numerous occurrences of oxidized ore. Oxidized zones extend to depths of at least 100 m below the present surface, and locally have economic concentrations of non-sulfide Zn-Pb ores referred to as "calamine ores." These calamine ores contain a mixture of supergene Zn (with minor Pb) carbonates (smithsonite), hydrated carbonates (hydrozincite), silicates (willemite) and hydrated silicates (hemimorphite, Zn clays) that cap the primary sulphide orebodies. Unlike most North African MVTs, this type of non-sulphide Zn ore deposits is largely confined to the central and eastern High Atlas Mountains (Goulet et al. 2014; present study). Such deposits are being extensively prospected by the mineral industry because (Sangster 2003): (1) environment impacts from mining are minimal owing to a characteristic lack of Pb, S, and other deleterious elements, (2) a potential for low-energy recovery of zinc, and (3) a generally higher in situ economic value (Borg 2002). According to our compilations, between 4,000 and 9,000 t of calamine ore are produced annually from the Jbel Bou Dahar district and adjacent deposits, at grades of 31–50 % Zn. Based on these estimates, a total of 220,000 to ~500,000 t of calamine ore have been produced since the 1970s when the CADETAF semi-private company in charge of selling the Pb–Zn ore from Jbel Bou Dahar, was created.

The sequence of mineral deposition shows the existence of five successive and overlapping stages of mineralization, almost all of which are of economic interest. These five stages are distinguished by megascopic and microscopic textural and cross-cutting relationships and mineral assemblages. Although an idealized paragenetic sequence is clearly identified throughout the district, there are variations in the abundance of minerals of particular stage from deposit to deposit, and even within the same deposit. Except for stage I that is barren, the rest of the paragenetic stages are of economic interest.

Stage I, the oldest hydrothermal stage, consists of pre-ore sparry calcite (Ca-1) and pyrite (Py-1), and is thought to record the earliest introduction of hydrothermal fluids into the district. Iron sulphides occur as fine disseminations of pyrite and marcasite dispersed within local host rocks, or as thin selvages coating rock porosity or clasts within breccias.

Stage II, referred to as the "main sulphide Pb–Zn stage ore," is economically the most important and accounts for more than 70 % of the Pb–Zn resources. The mineral paragenesis consists of variable proportions of galena and sphalerite with minor pyrite and chalcopyrite, accompanied by calcite (Ca-2) as the main gangue mineral.

Stage III is locally referred to as "Alquifoux" sulphide ore and constitutes for local miners the most attractive ore stage from which well-developed cubic and octahedral galena crystals (Gn-3) up to 12 cm across are being recovered. This stage matches the "cubo-octahedral stage" commonly described in MVTs worldwide (Bouabdellah et al. 2012).

Stage IV represents the late deposition of barite, celestite, and calcite (Ca-3), which are typically the last minerals deposited throughout the paragenesis, within the remaining open spaces near the Pb–Zn orebodies.

Stage V comprises later alteration, probably of supergene origin, of earlier stages that formed the most characteristic and commercially attractive mineral paragenesis in the district referred to as "calamine" or "non-sulphide Zn-Pb ore." This stage consists predominantly of an exotic mixture of smithsonite, hemimorphite, and hydrozincite together with calcite, and quartz. Calamine ores occur both as cavity fillings and as partial to massive replacements of host carbonates in the upper levels of the exploited orebodies. It seems that their genesis benefited from the interplay among weathering, uplift, and erosion and that there is no apparent relationship to the present water table (Goulet et al. 2014).

4.5 Fluid Inclusion Microthermometry

Microthermometric data from pre-ore hydrothermal calcite and various generations of sphalerite and barite display wide ranges in homogenization temperatures and related salinities, with T_h values ranging from <70° to 180 °C and salinities from ca. 15–26 wt percent NaCl equiv (Adil et al. 2004; Rddad and Bouhlel 2016). The similarity of fluid compositions in pre-ore hydrothermal calcite and sphalerite indicates homogeneity of the parent mineralizing fluid, and suggests that these two investigated minerals are genetically related and precipitated from the same hydrothermal system.

The measured Cl/Br and Na/Br molar ratios indicate that the mineralizing brines acquired high salinities and Ca/Na ratios through evaporation of seawater, and by subsequent dolomitization and fluid-rock interactions (Adil et al. 2004). Calculated fluid pressures in the range of 150–200 bars indicate depths of less than 1 km during ore deposition.

4.6 Sulphur and Lead Isotopes

Sulphur isotope compositions for various generations of sulphides from the Jbel Bou Dahar district show a wide range of $\delta^{34}S$ values from −1.2 to + 10.0 ‰ (Adil 2004). The highest values correspond to sulphides from the early Zn-rich stage I, whereas the lowest ratios are from the late cuboctahedral stage III. Secondary gypsum, interpreted to have resulted from supergene oxidation of preexisting sulphides, has $\delta^{34}S$ ratios of +4.5 to +9.6 ‰ (mean = 6.2 ‰, σ = 2.4 ‰, n = 4). Conversely, sulphur isotope compositions of the paragenetically late barite, with $\delta^{34}S$ values from 15.8 to 20.2 ‰ (mean = + 18.6 ‰, σ = 1.6 ‰, n = 7; Adil 2004), are within the range for Jurassic-Cretaceous seawater sulphate (∼10–23 ‰; Claypool et al. 1980; Kampschulte and Strauss 2004). This similarity suggests that the barite-hosted sulphur was derived from coeval seawater sulphate, either directly from the ocean or indirectly from leaching of marine evaporites. Celestite mineral separates exhibit the highest sulphur isotopic compositions with $\delta^{34}S$ values ranging from 16.3 to 27.5 ‰ (mean = 21.1 ‰, σ = 5 ‰, n = 5; Adil 2004).

Overall, the $\delta^{34}S$ values of sulphides (i.e., pyrite, sphalerite, and galena) are uniformly lower than the range of Jurassic seawater sulphate (∼10–23 ‰; Claypool et al. 1980; Kampschulte and Strauss 2004). More interestingly, the distribution of sulphur isotope compositions displays a general trend toward lower $\delta^{34}S_{sulphide}$ values with time (i.e., advancing paragenetic sequence) both at deposit and hand-sample scales. These large variations in sulphide $\delta^{34}S$ values from positive to negative are, therefore, interpreted to reflect isotopic fractionation during TSR and/or BSR of seawater sulphate or of pore seawater, at different rates of sulphate availability (open versus closed reservoirs with respect to sulphate) (Basuki et al. 2008; Vikre et al. 2011).

Indeed, the positive $\delta^{34}S_{sphalerite}$ values of the paragenetically early Zn-rich ore-stage (10–1 ‰; Adil 2004; Rddad and Bouhlel 2016) are consistent with rapid TSR of Mesozoic seawater sulphate or of dissolved pore-water sulphate. Conversely, the lower $\delta^{34}S_{galena}$ values of stages II and III (−1.2 to +7.8 ‰) fit within the range of values that record a system partially open to sulphate (Ohmoto et al. 2006; Basuki et al. 2008; Vikre et al. 2011).

Lead isotope compositions of galena performed in the course of the present study (Table 1; Fig. 11) plot in a tight cluster above the evolution curve of Stacey and Kramers (1975), with uniform $^{206}Pb/^{204}Pb$, $^{207}Pb/^{204}Pb$, and $^{208}Pb/^{204}Pb$ ratios from 18.111 to 18.205, 15.613 to 15.628, and 38.376 to 38.442, respectively. Compared to the Touissit and Mibladen Pb isotope compositions, the data for the Jbel Bou Dahar deposits fall precisely on the cluster of values shown by the Mibladen ore (Fig. 11), indicating again the derivation of Pb and by inference associated metals from a crustal source.

4.7 Age of Mineralization

The timing of MVT mineralization in the Jebel Bou Dahar district is poorly constrained because

of the lack of reliable geochronological data. Geological and paragenetic relationships indicate that the MVT deposits are clearly epigenetic and structurally controlled, and that the dolomitized host rocks were buried and lithified prior to the mineralizing event. Moreover, there is an intimate relationship between the ENE- and WSW-trending faults and the sites of MVT orebodies. Together, these relationships indicate that the Jbel Bou Dahar MVT mineralization formed as a result of hydrothermal processes initiated during deep burial by the compression and uplift during the Atlasic orogeny.

Textural relationships indicate that the mineralization post-dates compactional stylolites and therefore constrains the mineralizing event to after initial burial at about >600 m depth which occurred during the Cretaceous time. Consequently, a Cretaceous age (~100 Ma) can be used as a maximum time for mineralization. Furthermore, the strongly deformed nature of the ore suggests that the Jbel Bou Dahar mineralization took place shortly before, or during, the main pulse of the Atlasic orogeny, which is thought to have occurred in mid-Tertiary time (Frizon de Lamotte et al. 2009). Based on these constraints, it is thus concluded that the MVT mineralization in the Jbel Bou Dahar district occurred between the Cretaceous and Late Miocene, at the same time span during which the MVT deposits of the Touissit-Bou Beker and Mibladen districts formed.

4.8 Preliminary Genetic Model

Combined mineralogical, fluid inclusion, and geochemical data discussed above suggest that the Jbel Bou Dahar MVT deposits formed in mid- to late Tertiary time in response to large-scale crustal processes triggered by the Atalsic orogeny. The spatial link between the ENE- and WSW-trending faults and the sites of MVT orebodies implies that regional and local-scale faults played a crucial ore control by focusing fluid flow. Such spatial relationships and the occurrence of Pb–Zn mineralization in the Paleozoic basement rocks beneath the Liassic MVT host rocks (Adil 2004) requires an upward component of fluid flow (Fig. 14).

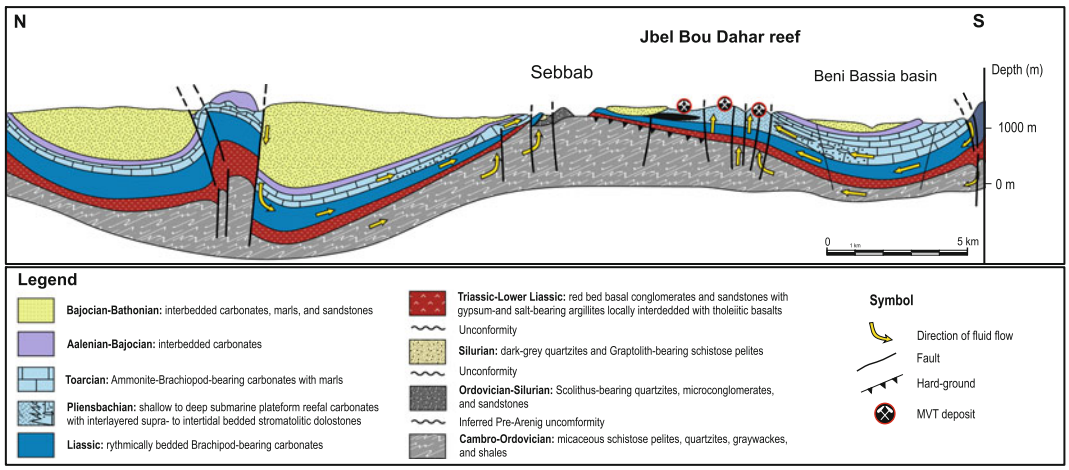

Fig. 14 N–S cross section illustrating compaction- and/or topographically driven fluid flow models for Jbel Bou Dahar hydrothermal fluids. Models invoke either (1) expulsion of hydrothermal fluids by compaction of sediments in depocenters, with sub-vertical faults acting as conduits for metal-bearing fluids under artesian conditions, or (2) transport of formation waters recharged in uplifted orogenic flank of Atlasic orogen, through early Mesozoic carbonate aquifer to Jbel Bou Dahar reef complex in mid-Tertiary time. Flow paths of fluids and waters are shown schematically by curved yellow arrows. Toarcian shales and Aalenian lime mudstones cap the early Liassic carbonate aquifer

The occurrence of mineralized veins within the Paleozoic basement rocks, and the unconformably overlying Aalenian-Bajocian marl and argillite cap rocks that likely forced ascending mineralizing brines to spread laterally to replace the more porous reefal facies of the Liassic strata, together indicate vertical fluid flow. This model is consistent with the vertical metal zoning that characterizes the Jbel Bou Dahar district. Similarly, the presence of sulphide orebodies within different lithologies, coupled with the succession of several episodes of brecciation, suggest that sulphide deposition was controlled largely by intrinsic characteristics of the host rocks, mainly permeability and porosity, and that the mineralizing fluids were introduced episodically.

Moreover, fluid inclusion data (Adil et al. 2004) indicate that multiple fluids were involved in forming the Jbel Bou Dahar deposits including saline formation brines, meteoric water, and mixed fluids. More interestingly, the linear distribution of homogenization temperatures and related salinities shown by Adil et al. (2004) is attribute to mixing and fluid-rock interaction between at least two distinct fluid types having contrasting salinities and Ca/(Ca + Mg) ratios: (1) an ascending warm (180 °C) and higher salinity (>25 wt% NaCl equiv), deep-seated, basement-equilibrated, metal-rich mineralizing fluid; and (2) a downward penetrating, cooler (70 °C), and lower salinity (16 wt% NaCl equiv), shallow, surface-derived formation water probably of meteoric origin.

Abundance of colloform-textured sulphides that infil vugs and veins constitutes additional evidence for fluid mixing. The fine-grained nature of the ore and local occurrence of dendritic forms of sulphides (i.e., Sebbab deposit) are indicative of rapid growth (e.g., Hitzman and Beaty 1996), which again is consistent with fluid mixing. Higher grade orebodies occur where pre-ore ground preparation provided sufficient porosity and permeability for fluid mixing. Consistent with the fluid inclusion data and textural relationships, the distribution of lead and sulphur isotope compositions suggests that metals and reduced sulphur did not travel together in the same brine, but mixed at the site of ore deposition. Moreover, the lowering of $\delta^{34}S$ values with advancing paragenetic sequence indicates that the Jbel Bou Dahar hydrothermal system, initially dominated by crustal fluids, became open at shallower levels to infiltration of increasing amounts of meteoric water, and to their mixing with the deep saline fluids. Cooling and dilution of a metal- and reduced sulphur-bearing fluid will not produce extensive sulphide replacement ore and dissolution of the host rocks (Plumlee et al. 1994), as observed in Jbel Bou Dahar district. From the standpoint of the source of lead, and by inference of associated metals, Pb isotope compositions indicate crustal sources via leaching of local Paleozoic basement rocks and derived siliciclastic country rocks.

Mineralization is thought to have taken place between the Cretaceous and mid-Tertiary time after maximum burial, as attested by the occurrence of sulphides cutting horizontal stylolites, coincident with maximum compression and rapid uplift during the Atlasic orogeny. This inferred depositional age for the Jbel Bou Dahar district which is consistent with the time span proposed by Rddad and Bouhlel (2016) coincides with the time interval proposed for the formation of the Touissit-Bou Beker and Mibladen MVT deposits. Accordingly, we suggest that the migration of the metaliferous basinal brines was initiated by a combination of basin subsidence and subsequent uplift during or immediately after the Atlasic orogeny. Although topographically driven fluid migration would have provided the main driving mechanism for the mineralizing fluids, rapid deposition of the thick post-Liassic carbonate and shale sequences in the neighboring depocenters (i.e., Beni Bassia basin; Fig. 14) could have provided compaction-driven fluids for generating the Jbel Bou Dahar ore-forming system.

5 Concluding Remarks

Major Moroccan MVT deposits share many similarities in term of geological environment, alteration, mineral paragenesis, and ore controls. Indeed, all of the three districts described herein (i.e., Touissit-Bou Beker, Mibladen, Jbel Bou

Dahar) are hosted by Jurassic shelf carbonate rocks unconformably overlain by an impermeable Upper Jurassic sequence that acted as aquitards, "cap rocks." Overall, the mineral paragenesis consists of variable proportions of sphalerite and galena, accompanied by lesser pyrite-marcasite and chalcopyrite ± sulphosalts (i.e., tetrahedrite). Non-sulphide gangue minerals include different generations of saddle dolomite (Touissit-Bou Beker), calcite (Jbel Bou Dahar), and barite (Mibladen).

Among several key factors that controlled the localization of the Pb–Zn ores, a crucial role in focusing fluid flow along the basement-cover interface involved the development of uplifted paleogeographic structures (basement highs) above which the economic Pb–Zn orebodies occur. The geometry of the orebodies that parallel the alpine ENE–WSW- and E–W-trending faults indicates that these deep-rooted structures allowed mineralizing fluids to recharge the basin, flow through aquifers and adjacent source rocks, replace the more porous carbonate rocks, and deposit metals into open spaces. Moreover, the presence of mineralized structures within the Paleozoic basement rocks, together with the presence of the overlying Upper Jurassic cap rocks that forced the ascending mineralizing brines to spread laterally along the Lower and Middle Jurassic aquifer, record both vertical and lateral fluid flow.

Fluid inclusion measurements, together with Na–Cl-Br leachate data, indicate that the ore-forming fluids correspond to evolved NaCl–$CaCl_2$–KCl–$MgCl_2$, basin-derived, hot (100 ± 20 °C), saline (>20 wt% NaCl equiv) brines. Calculated pressures for the ore fluids in the range of 150–200 bars suggest depths of less than 1 km for the Pb–Zn mineralization.

The absence of radiometric age constraints for ore formation constitutes the major obstacle to developing reliable genetic models. In this regard, field relationships together with Pb isotope data (Bouabdellah et al. 2012) indicate that the Moroccan MVT districts formed epigenetically during late Tertiary (Serravallian-Messinian) time, coincident with the major episode of Atlasic compression and uplift, and with the tectonic inversion of the Triassic-Jurassic basins in response to convergence of the African and Eurasian plates (Gieze and Jacobshagen 1992; Frizon de Lamotte et al. 2009). MVT mineralization is therefore interpreted to have resulted from the migration of deep metalliferous brines that were expelled either by (1) compaction of sediments in basin depocenters due to the rapid deposition of thick sequences of post-Liassic carbonate and shale (i.e., Jbel Bou Dahar district), or (2) a gravity-driven system (i.e., in all three districts) that provided the necessary hydrologic head for fluid movement, or (3) a combination of both processes. In the case of the Touissit-Bou Beker district, the main mineralizing event is attributed to the effects of extensional tectonics, Neogene-Quaternary mafic magmatism, and the Messinian salinity crisis (Bouabdellah et al. 2015). In this district, the associated elevated heat flow and subsequent increased geothermal gradient initiated buoyancy-driven fluid convection of downward-flowing Messinian seawater, which ultimately promoted the mobilization of older, high-temperature, rock-buffered basement brines stored within the Paleozoic basement, and the formation of base-metal-bearing chloride complexes. Mixing of Messinian seawater and basement-derived hydrothermal brines triggered deposition of the Pb- and Zn-rich ores (Bouabdellah et al. 2015).

References

Aboutahir N (1999) Pétrographie et géochimie des dolomites du district de Touissit-Bou Beker: hôte de la minéralisation de type de la Vallée du Mississippi (Maroc Nord-Oriental). Unpub PhD Thesis, Ecole Polytechnique, Montréal, Canada, 243 pp

Adil S (2004) Métallogenèse des gisements Pb–Zn de type Mississippi Valley de Jbel Bou Dahar (Haut Atlas Oriental, Maroc): apports des inclusions fluides et des isotopes de soufre. Unpub PhD Thesis, University Dhar El Mehraz, Fès, Morocco, 171 pp

Adil S, Bouabdellah M, Grandia F, Cardellach E, Canals A (2004) Caractérisation géochimique des fluides associés aux minéralisations Pb–Zn de Bou Dahar (Maroc). C R Geosci 336:1265–1272

Agard J, Du Dresnay R (1965) La région minéralisée du Jbel Bou Dahar, près de Beni Tajjit (Haut Atlas oriental): étude géologique et métallogénique. Notes Mem Serv Géol Maroc 181:135–166

Ajaji T, Weis D, Giret A, Bouabdellah M (1998) Coeval potassic and sodic calc-alkaline series in the post-collisional Hercynian Tanncherfi intrusive complex, northeastern Morocco: geochemical, isotopic and geochronological evidence. Lithos 45:371–393

Annich M, Rahhali M (2002) Gisement de plomb de Zeida. In: Barodi E-B, Watanabe Y, Mouttaqi A, Annich M (eds) Méthodes et techniques d'exploration minière et principaux gisements au Maroc. Projet JICA/BRPM, Bureau Recherche Participations Minières—BRPM, Rabat, pp 179–183

Appold MS, Garven G (1999) The hydrology of ore formation in the southeast Missouri district: numerical models of topography-driven fluid flow during the Ouachita orogeny. Econ Geol 94:913–935

Basuki NI, Taylor BE, Spooner ETC (2008) Sulfur isotope evidence for thermochemical reduction of dissolved sulfate in Mississippi Valley-type zinc-lead mineralization, Bongara area, northern Peru. Econ Geol 103:783–799

Beauchamp W, Barazangi M, Demnati A, El Alji M (1996) Intracontinental rifting and inversion: Missour Basin and Atlas Mountains, Morocco. AAPG Bull 80:1459–1482

Bethke CM (1986) Hydrologic constraints on the genesis of the Upper Mississippi Valley district from Illinois Basin brines. Econ Geol 81:233–249

Blomeier DPG, Reumer JJG (1999) Drowning of a Lower Jurassic carbonate paltform: Jbel Bou Dahar, High Atlas, Morocco. Facies 4:81–110

Blomeier DPG, Reijmer JJG (2002) Facies architecture of an Early Jurassic carbonate platform slope (Jbel Bou Dahar, High Atlas, Morocco). Jour Sed Research 72:462–475

Borg G (2002) The good, the bad, and the ugly—a maturity index for supergene non-sulfide zinc deposits [abs.]: Geol Soc America Abs Pgms 34:287

Bouabdellah M (1994) Métallogenèse d'un district de type Mississippi Valley, cas de Beddiane, district de Touissit-Bou Beker, Maroc. Unpub PhD Thesis, École Polytechnique, Montréal, Canada, 367 pp

Bouabdellah M, Héroux Y, Brown AC (1996a) Pétrographie et altération de la matière organique du gisement de plomb-zinc-cuivre de Beddiane, district de Touissit-Bou Beker, Maroc. Canad J Earth Sci 33:1363–1374

Bouabdellah M, Brown AC, Sangster DF (1996b) Mechanisms of formation of internal sediments at the Beddiane lead-zinc deposit, Touissit-Bou Beker mining district, northeastern Morocco. In: Sangster DF (ed) Carbonate-hosted lead-zinc deposits, society economic geologists, Spec Publ 4, pp 356–363

Bouabdellah M, Fontboté L, Haeberlin Y, Llinares L, Leach D, Spangenberg J (1999) Zoned sulphur isotope signatures at the Mississippi Valley-type Touissit-Bou Beker-El Abed district, Morocco, Algeria—evidence for thermochemical sulfate reduction and mixing of sulfur sources. In: Stanley C et al (eds) Mineral deposits: processes to processing, Fifth Bienn SGA Mtg and Fifth Quadrennial IAGOD Mtg, London, UK, 22–25 Aug 1999, pp 821–824

Bouabdellah M, Héroux Y, Chagnon A (2001) Zonation of organic matter reflectances and clay mineral assemblages around MVT deposits of Touissit-Bou Beker district, northeastern Morroco. In: Piestrzynski A, et al. (eds) Mineral deposits at the beginning of the 21st Century, 6th Bienn SGA Mtg, Krakow, Poland, 22–26 Aug 2001, pp 39–42

Bouabdellah M, Sangster DF, Leach DL, Brown AC, Johnson CA, Emsbo P (2012) Genesis of the Touissit-Bou Beker Mississippi Valley-type district (Morocco-Algeria) and its relationships to the Africa-Europe collision. Econ Geol 107:117–146

Bouabdellah M, Niedermann S, Velasco F (2015) The Touissit-Bou Beker Mississippi Valley-type district of northeastern Morocco: relationships to the Messinian salinity crisis, Late Neogene-Quaternary alkaline magmatism, and buoyancy-driven fluid convection. Econ Geol 110:1455–1484

Campbell AE, Stafleu J (1992) Seismic modeling of an early jurassic, drowned carbonate platform: Djebel Bou Dahar, High Atlas, Morocco. AAPG Bull 76:1760–1777

Carpenter AB, Trout ML, Pickett EE (1974) Preliminary report on the origin and chemical evolution of lead-and-zinc-rich oil field brines in central Mississippi. Econ Geol 69:1191–1206

Cathles LM, Smith AT (1983) Thermal constraints on the formation of Mississippi Valley-type lead-zinc deposits and their implications for episodic basin dewatering and deposit genesis. Econ Geol 78:983–1002

Crevello PD (1990) Stratigraphic evolution of Lower Jurassic carbonate platforms: record of rift tectonics and eustatsy, central and eastern High Atlas, Morocco. Unpubl PhD Thesis, Colorado School of Mines, Golden, Colorado, USA, 457 pp

Claypool GE, Holser WT, Kaplan TR, Sakai H, Zak I (1980) The age curves of sulfur and oxygen isotopes in marine sulfate and their mutual interpretations. Chem Geol 28:199–260

Cumming GL, Richards JR (1975) Ore lead isotope ratios in a continuously changing Earth. Earth Planet Sci Lett 28:155–171

Dagallier G, Macaudiere JM (1987) Contrôles tectoniques des concentrations Pb-Ba en milieu carbonaté de Mibladen (Maroc). Bull Soc Geol France 8:387–394

Dahire M (2004) Le complexe plutonique de la Haute Moulouya (Meseta oriental, Maroc): evolution pétrologique et structurale. Unpubl PhD Thesis, Mohamed Ben Abdellah University, Fès, Morocco, 322 pp

Dresnay Du R (1979) Sédiments jurassiques du domaine des chaines atlasiques du Maroc. Association des

Sédimentologistes Français (ASF) Spec Publ 1, pp 345–365

Duggen S, Hoernle K, van den Bogaard P, Garbe-Schönberg D (2005) Post collisional transition from subduction- to intraplate-type magmatism in the westernmost Mediterranean: evidence from continental-edge delamination of subcontinental lithosphere. J Petrol 46:1115–1201

Duggen S, Hoernle K, Hauff F, Klügel A, Bouabdellah M, Thirlwall MF (2009) Flow of Canary mantle plume material through a subcontinental lithospheric corridor beneath Africa to the Mediterranean. Geology 37:283–286

Dupuy JJ, Touray JC (1986) Multi-stage ore deposition at the Oued Mekta strata-bound lead deposit, Touissit-Bou Beker district, eastern Morocco. Econ Geol 81:1558–1561

Duthou JL, Emberger A, Lasserre M (1976) Résultats graphiques et interprétation de mesures isotopiques du plomb de galènes et des minéraux oxydés du Maroc. Soc Géol France 7:221–226

Ellouz N, Patriat M, Gaulier JM, Bouatmani R, Saboundji S (2003) From rifting to Alpine inversion: Mesozoic and Cenozoic subsidence history of some Moroccan basins. Sedimen Geol 156:185–212

Emberger A (1965) Eléments pour une synthèse métallogénique du district plombifère de la Haute Moulouya. Notes Mém Serv Géol Maroc 181:235–238

Evans I, Kendall CG (1977) An interpretation of the depositional setting of some deep-water Jurassic carbonates of the central High Atlas Mountains, Morocco. In: Cook HE, Enos P (eds) Deep-water carbonate environments, SEPM Spec Publ 25, pp 249–261

Fauquette S, Suc J-P, Bertini A, Popescu S-M, Warny S, Bachiri Taoufiq N, Perez Villa M-J, Chikhi H, Feddi N, Subally D, Clauzon G, Ferrier J (2006) How much did climate force the Messinian salinity crisis? Quantified climatic conditions from pollen records in the Mediterranean region. Palaeogeogr, Palaeoclimatol, Palaeoecol 238:281–301

Fedan B, Laville E, Mezgueldi AE (1989) Le bassin jurassique du Moyen Atlas (Maroc): exemple de bassin sur relais de décrochements. Bull Soc Géol France 5(6):1123–1136

Felenc R, Lenoble JP (1965) Le gîte de plomb de Mibladen. In: Colloque sur les gisements stratiformes de plomb, zinc et manganèse du Maroc. Notes Mem Serv Géol Maroc 181:185–204

Filali F, Guiraud M, Burg J-P (1999) Nouvelles données petro-structurales sur la boutonnière d'Aouli (Haute Moulouya): leurs conséquences sur la géodynamique hercynienne du Maroc. Bull Soc Géol France 4:435–450

Fiechtner L, Friedrichsen H, Hammerschmid K (1992) Geochemistry and geochronology of arly Mesozoic tholeiites from central Morococo. Geol Rundschau 81:45–62

Frizon de Lamotte D, Leturmy P, Missenard Y, Khomsi S, Ruiz G, Saddiqi O, Guillocheau F, Michard A (2009) Mesozoic and Cenozoic vertical movements in the Atlas system (Algeria, Morocco, Tunisia): an overview. Tectonophys 475:9–28

Garven G (1995) Continental-scale groundwater flow and geologic processes. Ann Review Earth Planet Sci 23:89–117

Ge S, Garven G (1992) Hydromechanical modeling of tectonically driven groundwater flow with application to the Arkoma foreland basin. J Geophys Res 97 (B6):9119–9144

Giese P, Jacobshagen V (1992) Inversion tectonics of intracontinental ranges: High and Middle Atlas, Morocco. Geol Rundschau 81:249–259

Gomez-Rivas E, Corbella M, Martín-Martín JD, Stafford SL, Teixell A, Bons PD, Griera A, Cardellach E (2014) Reactivity of dolomitizing fluids and Mg source evaluation of fault-controlled dolomitization at the Benicàssim outcrop analogue (Maestrat Basin, E Spain). Marine Petrol Geol 55:26–42

Goulet F, Charles N, Barbanson L, Branquet Y, Sizaret S, Annaciri A, Badra L, Chen Y (2014) Non-sulfide zinc deposits of the Moroccan High Atlas: multi-scale characterization and origin. Ore Geol Rev 56:115–140

Harmand C, Cantagrel JM (1984) Le volcanisme alcalin Tertiaire et Quaternaire du moyen Atlas (Maroc): chronologie K/Ar et cadre géodynamique. J Afr Earth Sci 2:51–55

Haynes FM, Kesler SS (1987) Chemical evolution of brines during Mississippi Valley-type mineralization: evidence from East Tennessee and Pine Point. Econ Geol 82:53–71

Hitzman MW, Beaty DW (1996) The Irish Zn-Pb orefield. In: Sangster DF (ed) Carbonate-hosted lead-zinc deposits. Soc Economic Geologists Spec Publ 4, pp 356–363

Hsü KJ, Cita MB, Ryan WBF (1973) The origin of the Mediterranean evaporites. Initial Repts Deep Sea Drilling Project 13:1203–1231

Jacobshagen VH, Gorler K, Giese P (1988) Geodynamic evolution of the Atlas system (Morocco). In: Jacobshagen VH (ed) The Atlas system of Morocco, Springer-Verlag, Berlin-Heidelberg-New York, Lecture Notes Earth Sci 15, pp 481–499

Jahn S, Bode R, Lyckberg P, Medenbach O, Lierl H-J (2003) Marokko-Land der Schönen Mineralien und fossilien. Bode Verlag GmbH, Salzhemmendorf, Germany 535 pp

Jébrak M, Marcoux E, Nasloubi M, Zahraoui M (1998) From sandstone- to carbonate-hosted stratabound deposits: an isotope study of galena in the Upper-Molulouya district (Morocco). Min Deposita 33:406–415

Jemmali N, Souissi F, Carranza EJM, Bouabdellah M (2013) Lead and sulfur isotope constraints on the genesis of the polymetallic mineralization at Oued

Maden, Jebel Hallouf and Fedj Hassene carbonate-hosted Pb–Zn (As–Cu–Hg–Sb) deposits, northern Tunisia. J Geochem Explor 132:6–14

Jenkyns HC, Jones CE, Grocke DR, Hesselbo SP, Parkinson DN (2002) Chemostratigraphy of the Jurassic system: applications, limitations and implications for palaeoceanography. J Geol Soc 159:351–378

Kampschulte A, Strauss H (2004) The sulfur isotope evolution of Phanerozoic seawater based on the analysis of structurally substituted sulfate in carbonates. Chem Geol 204:255–286

Kendrick MA, Burgess R, Leach DL, Pattrick RAD (2002a) Hydrothermal fluid origins in Mississippi Valley-type ore districts: combined noble gas (He, Ar, Kr) and halogen (Cl, Br, I) analysis of fluid inclusions from the Illinois-Kentucky fluorspar district Viburnum Trend and Tri-State districts, Midcontinent United States. Econ Geol 97:453–469

Kendrick MA, Burgess R, Pattrick RAD, Turner G (2002b) Hydrothermal fluid origins in a fluorite-rich Mississippi Valley-type district: combined noble gas (He, Ar, Kr) and halogen (Cl, Br, I) analysis of fluid inclusions from the South Pennine ore field, United Kingdom. Econ Geol 97:435–451

Kenter J, Campbell AE (1991) Sedimentation on a Lower Jurassic carbonate platform flank: geometry, sediment fabric and related depositional structures (Djebel Bou Dahar, High Atlas, Morocco). Sedimen Geol 72:1–34

Kontak DJ, Sangster DF (2005) Aqueous and liquid petroleum inclusions in barite from the Walton deposit, Nova Scotia, Canada: a Carboniferous, carbonate-hosted Ba–Pb–Zn–Cu–Ag deposit. Econ Geol 93:845–868

Krijgsman W, Langereis CG, Zachariasse WJ, Boccaletti M, Moratti G, Gelati R, Iaccarino S, Papani G, Villa G (1999) Late Neogene evolution of the Taza-Guercif basin (Rifian corridor, Morocco) and implications for the Messinian salinity crisis. Marine Geol 153:147–160

Kucha H, Schroll E, Raith JG, Halas S (2010) Microbial sphalerite formation in carbonate-hosted Zn-Pb ores, Bleiberg, Austria: micro- to nanotextural and sulfur isotope evidence. Econ Geol 105:1005–1023

Leach DL, Sangster DF (1993) Mississippi Valley-type lead-zinc deposits. In: Kirkham RV, Sinclair WD, Thorpe RI, Duke JM (eds) Mineral deposit modeling. Geol Assoc Can Spec Paper 40, pp 289–314

Leach DL, Bradley DC, Huston D, Pisarevsky SA, Taylor RD, Gardoll SJ (2010) Sediment-hosted lead-zinc deposits in Earth history. Econ Geol 105:593–625

Lustrino M, Wilson M (2007) The circum-Mediterranean anorogenic Cenozoic igneous province. Earth-Sci Rev 81:1–65

Makhoukhi S (1993) Le gisement de plomb de Beddiane (Maroc oriental): gîtologie et éléments de modélisation d'une minéralisation de type Mississippi Valley. Unpub PhD Thesis, École Normale Supérieure Paris, 124 pp

Makhoukhi S, Marignac Ch, Pironon J, Schmitt JM, Marrakchi C, Bouabdelli M, Bastoul A (2003) Aqueous and hydrocarbon inclusions in dolomite from Touissit-Bou Beker district, eastern Morocco: a Jurassic carbonate hosted Pb–Zn(Cu) deposit. J Geochem Explor 78–79:545–551

Merino-Tomé O, Della Porta G, Kenter JAM, Verwer K, Harris PM, Adams E-W, Playton T, Corrochano D (2012) Sequence development in an isolated carbonate platform (Lower Jurassic, Djebel Bou Dahar, High Atlas, Morocco): influence of tectonics, eustacy and carbonate production. Sedimentol 59:118–155

Naji M (2004) Les minéralisations plombo-barytiques du district de la Haute Moulouya. Contexte géologique, contrôle tectonique et modèle de mise en place: gisements d'Aoul-Mibladen-Zeida. Unpub PhD Thesis, Mohammed V University, Rabat, Morocco, 218 pp

Ohmoto H, Watanabe Y, Ikemi H, Poulson SR, Taylor BE (2006) Sulphur isotope evidence for an oxic Archaean atmosphere. Nature 442:908–911

Oliver J (1986) Fluids expelled tectonically from orogenic belts: their role in hydrocarbon migration and other geologic phenomena. Geology 14:99–102

Ouarhache D, Charrière A, Charlot-Prat F, El Wartiti M (2012) Chronologie et modalities du rifting triassico-liasique à la marge sud-ouest de la Téthys alpine (Moyen Atlas et Haute Moulouya, Maroc); corrélation avec le rifting Atlantique: simultanéité et diachronisme. Bull Soc Geol France 183:233–249

Oukemini D, Bourne J, Krogh TE (1995) Géochronologie U-Pb sur zircon du pluton d'Aouli, Haute Moulouya, Maroc. Bull Soc Geol France 166:15–21

Owodenko B (1976) Le bassin houiller de Jerada (Maroc oriental). Notes Mem Serv Géol Maroc 207, 147 pp

Plumlee GS, Leach DL, Hofstra AH, Landis GP, Rowan EL, Viets JG (1994) Chemical reaction path modeling of ore deposition in Mississippi Valley-type Pb–Zn deposits of the Ozark region, U.S. Mid-continent. Econ Geol 89:1361–1383

Praszkier T (2013) Mibladen, Morocco. Mineral Record 44:247–285

Rahhali M (2002) Gisements stratiformes de Mibladen. In: Barodi E-B, Watanabe Y, Mouttaqi A, Annich M (eds) Méthodes et techniques d'exploration minière et principaux gisements au Maroc. Projet JICA/BRPM, Bureau Recherche Participations Minières—BRPM, Rabat, pp 166–170

Rajlich P (1983) Geology of Oued Mekta, a Mississippi Valley-type deposit, Touissit-Bou Beker region, eastern Morocco. Econ Geol 78:1239–1254

Rddad L, Bouhlel S (2016) The Bou Dahar Jurassic carbonate-hosted Pb–Zn–Ba deposits (Oriental High Atlas, Morocco): fluid-inclusion and C–O–S–Pb isotope studies. Ore Geol Rev 72:1072–1087

Samson P (1973) Un gisement plombo-zincifère en milieu récifal: Touissit (Maroc oriental). Notes Mém Service Géol Maroc 242, 133 pp

Sangster DF (2003) A special issue devoted to nonsulfide zinc deposits: a new look. Econ Geol 98:683–684

Scheibner C, Reumer JJG (1999) Facies patterns within a Lower Jurassic upper slope to inner platform transect (Jbel Bou Dahar, Morocco). Facies 41:55–80

Sharp JM (1978) Energy and momentum transport model of the Ouachita basin and its possible impact on formation of economic mineral deposits. Econ Geol 73:1057–1068

Sheppard SMF (1986) Characterization and isotopic variations in natural waters. In: Valley JW, Taylor HP Jr, O'Neil JR (eds) Stable isotopes in high temperature geological processes. Mineral Soc Am Rev Mineral 16:165–184

Stacey JS, Kramers JC (1975) Approximation of terrestrial lead isotope evolution by a two-stage model. Earth Planet Sci Lett 26:207–221

Torbi A, Gélard JP (1994) Paléocontraintes enregistrées par la microfracturation, depuis l'Hercynien jusqu'à l'Actuel, dans les Monts du Sud-Est d'Oujda (Meseta orientale, Maroc). C R Acad Sci Paris 318:131–135

Torbi A (1996) Stratigraphie et évolution structurale paléozoïque d'un segment de la Meseta orientale marocaine (Monts du Sud-Est d'Oujda): rôle des décrochements dans la formation de l'olistostrome intraviséen et le plutonisme tardi-hercynien. Jour Afr Earth Sci 22:549–563

Touahri B (1991) Géochimie et métallogénie des minéralisations à Pb et Zn du nord de l'Algérie. Mémoire du Service Géologique d'Algérie No. 4, 260 pp

Ulrich MR, Bodnar RJ (1988) Systematics of stretching of fluid inclusions II: barite at 1 atm confining pressure. Econ Geol 83:1037–1046

Valin F, Rakus M (1979) Rapport concernant l'étude géologique du Paléozoique et de la couverture mésozoique dans les Monts d'Oujda. Unpub Rept, Service Géologique d'Oujda 60, 73 pp

Vauchez A (1976) Les déformations anté-triasiques dans la boutonnière d'Aouli-Mibladen. C R Acad Sci Paris 282:425–428

Vikre PG, Poulson SK, Koenig AE (2011) Derivation of S and Pb in Phanerozoic intrusion-related metal deposits from Neoproterozoic sedimentary pyrite, Great Basin, United States. Econ Geol 106:883–912

Vitrac AM, Albarede F, Allègre CJ (1981) Lead isotopic composition of Hercynian granitic K-feldspars constrains continental genesis. Nature 291:460–464

Voirin J (1965) Géologie du gisement plombo-zincifère de Bou Beker. In: Colloque sur les gîtes stratiformes de plomb, zinc et manganèse du Maroc 1962. Notes Mémoires Service Géologique Maroc 181:21–68

Warme JE (1988) Jurassic carbonate facies of the central and eastern High Atlas rift, Morocco. In: Jacobshagen V (ed) The Atlas system of Morocco, Springer-Verlag, Berlin-Heidelberg-New York, Lecture Notes Earth Sci 15, pp 169–199

Wittig N, Pearson DG, Baker J, Duggen S, Hoernle K (2010) A major element, PGE and Re-Os isotope study of Middle Atlas (Morocco) peridotite xenoliths: evidence for coupled introduction of metasomatic sulphides and clinopyroxene. Lithos 115:15–26

Zartman RE, Doe BR (1981) Plumbotectonics—the model. Tectonophys 75:35–162